Politecnico di Torino

Master's degree program in
ENVIRONMENTAL AND LAND ENGINEERING

Earth Observation Methodology in Carbon Credit Domain

Supervisor:
professor Piero Boccardo

Candidate:
Jamal Khademi
S302606

A.a. 2023/2024
October 2024

Acknowledgments

I would like to express my sincere gratitude to my supervisor, **Professor Piero Boccardo**, for his invaluable guidance, patience, and insightful feedback throughout the development of this thesis. His expertise in the field of remote sensing and environmental engineering has been instrumental in shaping my research.

I am also thankful to the faculty of the **Politecnico di Torino**, particularly the department of Environmental and Land Engineering (**DIATI**), for providing me with the resources and support needed to complete this work.

Finally, I would like to thank my family for their unwavering support and belief in me, without which this accomplishment would not have been possible.

Table of Contents

Abstract

Overview of Carbon Sequestration

Carbon sequestration is the process of capturing and storing atmospheric carbon dioxide (CO2). It is one of the most promising methods to mitigate the increasing levels of greenhouse gases in the atmosphere, which are contributing to global climate change. Forests, soils, and oceans are natural carbon sinks where this CO2 is stored. Various techniques such as afforestation, reforestation, and soil management practices play a crucial role in capturing carbon. Remote sensing technologies provide a cost-effective and scalable way to monitor these carbon sequestration efforts across large areas.

Relevance in Climate Mitigation and Carbon Trading

As the world seeks solutions to mitigate the impact of climate change, carbon trading has emerged as an important market mechanism under the Paris Agreement. Carbon credits represent the reduction or removal of CO2 emissions, and they can be traded in both compliance and voluntary markets. Remote sensing technologies allow for accurate estimation of carbon stocks, enabling verification of carbon credits and supporting the carbon trading system. Effective monitoring of carbon sequestration is essential for maintaining transparency and integrity in carbon markets.

Remote Sensing's Role in Carbon Stock Estimation

Remote sensing technologies, particularly satellite-based methods, play a key role in estimating carbon stocks by providing detailed, frequent, and reliable data. These methods allow for the monitoring of vegetation health, land-use changes, and biomass estimation, which are critical for assessing carbon sequestration potential. With the development of new sensors and satellite missions like Landsat and Sentinel, the capacity to monitor carbon stocks at a global scale has improved significantly.

Current Methods of Biomass and Carbon Stock Estimation

Biomass estimation has traditionally been carried out through ground-based field measurements, but these are costly and time-consuming, making remote sensing a more feasible option for large-scale estimations. Common methods involve the use of vegetation indices such as the Normalized Difference Vegetation Index (NDVI), Enhanced Vegetation Index (EVI), and other spectral data obtained from satellites. These indices are used to correlate the amount of vegetation cover with carbon content.

Vegetation Indices in Carbon Stock Assessment

Vegetation indices like NDVI and EVI have been widely used for estimating vegetation biomass and carbon stocks. NDVI is particularly useful for detecting the presence and health of vegetation, while EVI enhances sensitivity to areas with high biomass. However, the effectiveness of these indices varies depending on the vegetation type, seasonality, and environmental conditions. Calibration with ground-based measurements is often required for more accurate assessments.

Challenges in Biomass Estimation

Using Remote Sensing Despite the advancements in remote sensing, several challenges remain in accurately estimating biomass and carbon stocks. These include the complexity of vegetation structure, seasonal variations, cloud cover, and the varying spatial resolutions of satellite imagery. Additionally, the relationship between vegetation indices and biomass is not always linear, requiring further calibration and validation through ground-truthing techniques.

Methodology and Data Analysis

Satellite Processing

In this study, the processing of satellite imagery from Sentinel-2, Landsat 8, and Landsat 9 was performed to derive vegetation indices and classify land cover types within the specified study area. The focus was on generating and analyzing time-series data using the Normalized Difference Vegetation Index (NDVI) and the Enhanced Vegetation Index (EVI) for 2023.

Geometry

Sentinel-2 Processing:

- Sentinel-2 imagery was filtered based on the date range from January 1, 2023, to December 31, 2023. The filtering criteria included the removal of images with cloud coverage exceeding 10%.
- Selected images were processed to retain only relevant bands: Blue (B2), Green (B3), Red (B4), Near Infrared (B8), Shortwave Infrared 1 (B11), and Shortwave Infrared 2 (B12). These bands were scaled using a factor of 0.0001 to convert the reflectance values to the appropriate range.
- Vegetation indices were computed using the scaled bands. NDVI was derived from the NIR (B8) and Red (B4) bands using the formula: NDVI = (NIR - Red) / (NIR + Red).
- EVI was calculated using the NIR (B8), Red (B4), and Blue (B2) bands with the formula: EVI = 2.5 * (NIR - Red) / (NIR + 6 * Red - 7.5 * Blue + 1).

Landsat 8 and Landsat 9 Processing:

• For Landsat 8 and Landsat 9, the imagery was filtered to include data from the same date range and with cloud coverage less than 10%.

• The relevant bands for Landsat 8 (B1, B2, B3, B4, B5, B6, B7) and Landsat 9 (B1, B2, B3, B4, B5, B6, B7) were scaled to reflectance values using a factor of 0.0000275 and an offset of -0.2.

• NDVI and EVI were computed similarly to Sentinel-2 using the scaled bands, with appropriate adjustments for the specific band names and scaling factors of Landsat 8 and Landsat 9.

Using NDVI and EVI

NDVI and EVI were employed in this analysis to monitor vegetation health and land cover changes. NDVI is a widely used vegetation index that is sensitive to chlorophyll content in plants, making it useful for assessing vegetation density and health. EVI, on the other hand, is designed to enhance the signal-to-noise ratio and reduce atmospheric influences, particularly in areas with dense vegetation. The combination of these indices provides a more comprehensive understanding of vegetation dynamics and land cover classification.

Computation of Monthly Time Series

To analyze temporal changes, monthly time series data were computed for both NDVI and EVI. The following steps were followed:

1. Creation of Monthly Composite Images:

The image collections for NDVI and EVI were filtered to select images from each month of the year.

For each month, a median composite was generated to minimize the impact of outliers and provide a representative measure of vegetation conditions.

2. Generation of Monthly Time Series:

The median images for each month were compiled into time series datasets for both NDVI and EVI, covering the full year of 2023.

The time series data were visualized to analyze seasonal patterns and variations in vegetation indices.

Validation Through Time Series NDVI

Validation was performed by comparing the NDVI data across different times of the year. The focus was on April and October, which represent typical spring and autumn conditions.

1. Comparison of April and October NDVI:

   NDVI composites for April and October were computed to assess seasonal variations in vegetation health.

   Thresholding was applied to classify different land cover types based on NDVI values, such as cropland, grassland, and tree cover.

2. Area Calculation and Analysis:

   The areas of different land cover types were calculated based on classified NDVI images for April and October. This was achieved by multiplying the binary classification images by pixel area and summing the results to obtain total areas in hectares.

3. Time Series Charts:

   Time series charts for NDVI and EVI were generated to analyze temporal changes and validate the accuracy of the classifications. These charts provided insights into vegetation trends over time and supported the interpretation of seasonal and annual variations.

Introduction

Overview of Carbon Sequestration

A mechanism designed to support the reduction of greenhouse gas emissions and promote sustainable development has been created under the oversight of the Conference of the Parties to the Paris Agreement. This system, available for voluntary participation by member countries, will be monitored by a designated body appointed by the Conference. Its primary objectives include:

(a) advancing efforts to lower greenhouse gas emissions while encouraging sustainable development.

(b) encouraging both public and private sector entities, as authorized by participating countries, to engage in emissions reduction activities.

(c) assisting in the reduction of emissions within host countries, which will benefit from these mitigation actions, with the possibility of transferring the resulting emission reductions to other nations to help meet their nationally determined contributions; and

(d) achieving a net decrease in global emissions.(Paris Agreement, n.d.)

It is important to note that the mechanism established under Article 6, paragraph 4, of the Paris Agreement can act as a reliable benchmark for international carbon crediting. This framework ensures environmental integrity, recognizing that carbon offsetting serves as a complement to the significant reductions in greenhouse gas emissions required globally.(Guidance on the Mechanism Established by Article 6, Paragraph 4, of the Paris Agreement, n.d.)

It has been decided that afforestation and reforestation projects, as well as programs previously registered under the Clean Development Mechanism (CDM), may transition to the mechanism outlined in Article 6, paragraph 4, of the Paris Agreement. These projects can be re-registered under the new mechanism, provided they meet the following conditions:

(a) A request to transition the CDM afforestation and reforestation project or program must be submitted to the secretariat and the CDM host Party, as defined by decision 3/CMP.1, by or on behalf of the project participants no later than June 30, 2024.

(b) The CDM afforestation and reforestation activity must comply with the applicable requirements for removal activities under the CMA 5 – Agenda item 14

(c) 3 mechanisms, as defined in Article 6, paragraph 4, of the Paris Agreement, as detailed in annex II and any additional relevant decisions made by the CMA.(Guidance on the Mechanism Established by Article 6, Paragraph 4, of the Paris Agreement, n.d.)

A tradable credit is awarded to a nation, company, or entity for reducing carbon dioxide or other greenhouse gas emissions by one metric ton below a designated emission threshold.(*Carbon Credit*, n.d.)

Incorporating forest carbon sinks into carbon trading systems provides a crucial solution to address the funding gap in emission reduction initiatives. It is also a key strategy for achieving carbon sequestration and moving toward carbon neutrality. A carbon credit trading mechanism is proposed, which is based on forest carbon sinks and optimized for forest companies and manufacturers. The scale of forest carbon sinks and the associated trading prices are determined using a stochastic differential game approach. By assigning appropriate emission reduction responsibilities, a balance can be struck between forest carbon sequestration and economic development. The findings suggest that companies with a long-term perspective are more inclined to engage in carbon credit trading when forest carbon sequestration levels are low, while those with a short-term outlook prefer trading when the sequestration potential is high. Furthermore, assigning lower emission reduction obligations in carbon trading promotes greater participation from short-term focused companies and increases overall forest carbon sequestration. This demonstrates the effectiveness of the proposed trading mechanism, highlighting that forest companies should take on lower emission reduction responsibilities to achieve both economic and environmental gains.(Song & Wu, 2023)

Relevance in Climate Mitigation and Carbon Trading

The global effort to mitigate climate change has increasingly emphasized the role of carbon trading as a market-based mechanism for reducing greenhouse gas emissions. This system facilitates the exchange of carbon credits, which represent a unit of emission reduction achieved through various projects and practices. By putting a price on carbon emissions, carbon trading incentivizes companies, governments, and organizations to engage in sustainable practices that contribute to a reduction in overall emissions.

Carbon Offsets and Carbon Credits

Although the terms "carbon credits" and "carbon offsets" are frequently used interchangeably, they represent two separate concepts with distinct functions. It is crucial to comprehend the differences between them before making any purchases, as understanding these distinctions can help you achieve your objectives. Below is a general definition of each term:

- Carbon offset: A removal of GHGs from the atmosphere.
- Carbon credit: A reduction in GHGs released into the atmosphere.

To illustrate the distinction, consider a water source contaminated by a nearby chemical facility. A “chemical offset” would involve removing pollutants from the water to cleanse it. In contrast, a “chemical

credit" would entail compensating another chemical company to reduce its emissions into the water, thereby maintaining the overall pollution level.

Let's take a closer look at each of these products individually. The process of creating a carbon offset is known as "carbon sequestration." This term is reminiscent of how a judge may sequester a jury, effectively isolating them from external influences.

Similarly, carbon offsets entail the removal of CO2 emissions from the atmosphere and their secure storage for a designated period.

A variety of methods exist for achieving carbon offsets, such as planting trees, breaking down rock into smaller particles, storing carbon in specialized devices, capturing methane from landfills, and the ultimate goal of carbon sequestration: employing advanced technologies to convert CO2 emissions into usable products.

Carbon offsets are generated by independent companies that extract CO2 from the atmosphere. These offsets are then sold to entities that emit (or have emitted) CO2. Thus, companies that produce offsets receive direct funding from those businesses responsible for greenhouse gas emissions.

Conversely, carbon credits are typically "issued" by government entities. Authorities establish limits on the amount of greenhouse gases that organizations can release by implementing caps—defining a specific tonnage of CO2 that a company is allowed to emit. Each ton of CO2 under this cap is considered a carbon credit.

Companies meet these caps by reducing their emissions through enhanced energy efficiency or transitioning to renewable energy sources. Any organization that successfully lowers its emissions below the legal requirement can sell its surplus credits to other businesses that find it challenging to reduce their own emissions to comply with regulations.

- **The Two Carbon Markets**

Another key distinction between carbon credits and carbon offsets is that carbon credits are typically traded in the compliance market, while carbon offsets are mainly exchanged in the voluntary carbon market.

As mandatory regulations to limit greenhouse gas emissions have increased, a fragmented carbon compliance market has begun to emerge. For instance, the European Union operates an Emissions Trading System (ETS), which allows companies to purchase carbon credits from other businesses.(Roh et al., 2014)

The voluntary carbon market, which focuses on offsets, is significantly smaller than the compliance market; however, it is projected to expand substantially in the coming years. This market is accessible to individuals, companies, and various organizations aiming to reduce or eliminate their carbon footprints, even if they are not mandated to do so by law.

Consumers can buy offsets for emissions generated by specific high-emission activities, such as a long-haul flight. Alternatively, they may opt to purchase offsets regularly to mitigate their ongoing carbon emissions.(Kazak et al., 2016)

How to produce carbon credits

A wide range of businesses can generate and sell carbon credits by implementing various processes to reduce, capture, and store emissions.

Some of the most common types of carbon offset projects include:

- Renewable energy projects,
- Improving energy efficiency,
- Carbon and methane capture and sequestration
- Land use and reforestation.

Renewable energy initiatives have been in place long before the emergence of carbon credit markets. Many nations are fortunate to possess abundant renewable energy resources. For instance, countries like Brazil and Canada, which are rich in lakes and rivers, or Denmark and Germany, known for their windy landscapes, have found renewable energy to be an appealing and cost-effective power generation method. These resources now also provide the added advantage of generating carbon offsets.

Improvements in energy efficiency further enhance renewable energy projects by lowering the energy requirements of existing buildings and infrastructure. Simple actions, such as replacing incandescent bulbs with LED lights in homes, can significantly reduce power consumption and benefit the environment. On a broader scale, this could involve upgrading buildings, optimizing industrial processes for greater efficiency, or providing more efficient appliances to underserved communities.

Carbon and methane capture entails implementing strategies that extract CO2 and methane—gases that are over 20 times more detrimental to the environment than CO2— from the atmosphere.

Methane is generally easier to manage, as it can be combusted to produce CO2. While this may initially seem counterproductive—given that methane is over 20 times more harmful to the atmosphere than CO2—burning one molecule of methane to convert it into CO2 can still result in a net emissions reduction of more than 95%.

For carbon capture, the process typically occurs directly at the source, such as in chemical or power plants. Although the underground injection of captured carbon has been employed for various applications, like enhanced oil recovery, for decades, the concept of long-term carbon storage—comparable to the handling of nuclear waste—is relatively new.

Land use and reforestation initiatives leverage nature's carbon sinks, namely trees and soil, to absorb atmospheric carbon. This encompasses efforts to protect and restore existing forests, establish new ones, and implement soil management practices.

Through photosynthesis, plants convert CO2 from the atmosphere into organic matter, which ultimately contributes to the soil as decomposed plant material. When this carbon-rich material is absorbed, it helps restore the soil's natural properties, enhancing crop productivity while minimizing pollution.(Reichle, 2023)

Crop seasonality

Cover crops are a vital management practice that can sustainably boost crop yields while also enhancing soil health and water quality. Usually sown in the fall following the harvest of cash crops, cover crops offer vegetative cover during the winter months. The environmental advantages they provide include controlling soil erosion, improving water infiltration, reducing runoff, decreasing weed and pest pressure, minimizing chemical leaching from fields, and promoting soil microbial activity. (Ahmed et al., 2023).

The introduction of advanced remote sensing technologies has enabled researchers to perform extensive field and large-scale studies more efficiently, often reducing costs and labor while enhancing overall data accuracy. Nevertheless, these remote sensing methods have limitations, including restricted temporal and spatial resolution, local cloud cover, and image gaps, which can complicate vegetation classification. Despite these challenges, the advantages of timely and cost-effective analyses often outweigh the drawbacks, particularly for the assessment of large areas.(Ahmed et al., 2023)

The advent of satellite technology has led to the creation of extensive datasets obtained through remote sensing, which are valuable for agriculture, environmental management, disaster response, navigation, and transportation. Multispectral sensors, which capture 3 to 10 broad bands, and hyperspectral sensors, which collect data across hundreds of narrow bands, have been incorporated into various satellite platforms, such as Landsat, Sentinel, and Unmanned Aerial Vehicles (UAVs), enhancing Earth observation capabilities. This technology allows for the monitoring of the spectral and temporal characteristics of agricultural land with high spatial and temporal resolution. The deployment of multiple satellites can help alleviate data gaps across specific temporal and geographic areas; however, a trade-off often exists between high spatial resolution (as seen with Sentinel) and high temporal resolution (as seen with Landsat). (Ahmed et al., 2023).

Climate change is profoundly affecting the growing seasons of terrestrial ecosystems, as rising temperatures result in alterations to the duration of these seasons. Such changes impact the exchanges of carbon, energy, and water between ecosystems and the atmosphere on a seasonal basis. Research indicates that earlier leaf emergence in spring can boost carbon uptake at the beginning of the growing season. However, this may lead to a reduction in carbon uptake later due to moisture constraints. Similarly, warmer autumns can heighten respiration rates while diminishing net carbon uptake. It is essential to comprehend how shifts in phenology will affect terrestrial carbon, energy, and water budgets, particularly since global ecosystems are interconnected with the climate system. (Lee et al., 2023).

Monitoring changes in cropland is essential for carbon credit systems; however, mapping these areas presents challenges due to their seasonal variations and human activities. Both large-scale mapping and change detection efforts depend on seasonal imagery, and the irregular distribution of Landsat data throughout the year can impact accuracy. Satellite sensors are adept at capturing consistent and

repeatable measurements, making them suitable for detecting a variety of change processes, including natural disturbances (such as fires and insect infestations) and human-induced changes (like deforestation, urbanization, and agricultural activities). (Jin & Sader, 2005).

Ecosystem changes can be categorized into three types: (1) seasonal changes driven by interactions between annual temperature and rainfall that impact plant phenology; (2) gradual changes resulting from interannual climate variability or alterations in land management practices; and (3) abrupt changes caused by disturbances such as deforestation, urbanization, floods, and wildfires. (Verbesselt et al., 2010).

Estimating changes using remotely sensed data is a complex process, as time series data contain a combination of seasonal, gradual, and abrupt changes, in addition to noise caused by geometric errors, atmospheric scattering, and cloud cover. (Roy et al., 2002).

Remote Sensing's Role in Carbon Stock Estimation

Remote sensing is the technique of obtaining information about an object, location, or event by analyzing data collected by a sensor that is not in direct contact with the subject being studied.(Manson et al., 2015). Remote sensing studies leverage data gathered from handheld devices, truck-mounted equipment, and other terrestrial instruments, as well as information obtained from various aerial and satellite platforms. Remote sensing cameras capture images that allow researchers to collect data about the Earth. This technique is effective for generating policy-relevant indicators that can inform various aspects of planning and management. It enables the collection of data from a distance, primarily using satellites or aircraft, to monitor and assess changes in the Earth's surface over time. (Janga et al., 2023).

Satellite imagery captures a series of photographs of a field to assess its condition, allowing for the implementation of measures aimed at improving crop productivity. For instance, sensors can act as an early warning system, enabling producers to quickly adopt management practices before problems escalate. Additionally, these technologies can perform basic plant counts, evaluate plant health, estimate crop yields, assess damage, manage irrigation, identify unwanted vegetation, detect signs of agricultural distress, prevent disasters, and create visual representations of the field. (Dhanaraju et al., 2022). Remote sensing technologies are currently progressing rapidly and have become more cost-effective for gathering data at the field level. To understand crop development throughout the growing season, it is essential to create maps that illustrate crop growth, the presence of diseases, weed occurrences, nutrient deficiencies, and other factors affecting crops and soil. As a result, maps generated from images captured through remote sensing, which showcase the diversity of crops and soil, have become vital tools in agriculture.

(Mulla, 2013).

Remotely sensed imagery can be applied in several key areas, including mapping soil properties, classifying crop species, detecting water stress in crops, monitoring weeds and diseases, and assessing crop yields. The choice of data collection platforms—whether satellite, aerial, or ground-based—affects how remote sensing is utilized. Furthermore, the sensor resolutions play a critical role in determining the number and width of the spectral bands captured (ranging from multispectral to hyperspectral), as well as the temporal (hourly, daily, weekly), spatial (high, medium, low), and radiometric (8-bit, 12-bit, 16-bit) characteristics. When using remotely sensed images for agricultural decision-making, it is essential to carefully consider several factors, including:

1) The level of alignment between the image and the actual ground location, commonly referred to as geometric accuracy.
2) The characteristics of the remote sensors, including their radiometric and geometric specifications and measurements.
3) The precision of the images in representing ground features, assessed in terms of both spatial and spectral resolutions.
4) The extent of spectral information represented in the captured images.
5) The availability of satellite imagery and the associated costs involved; and

6) The skill level of end-users in remote sensing technology and their ability to understand and integrate information into decision-making processes, among other factors.

Remote sensing technologies are crucial in agriculture, offering essential data and insights that improve decision-making and optimize various farming practices, primarily through the estimation of different indices. (Sarmin et al., 2024)

Below are some keyways in which remote sensing is integrated into agriculture:

1. **Land Use and Land Cover (LULC) Identification and Change Detection**: One of the primary applications of remote sensing data is in tracking land use and detecting changes. This information is vital for rural and urban planning, natural resource management, and environmental conservation, as it provides insights into changes in land use and land cover (LULCCs). LULC map analysis offers a quick and accurate summary of green vegetation assessments and soil characteristics. Satellite imagery facilitates regular monitoring of land surfaces, enabling the mapping of crop health, stormwater runoff, air quality, environmental evaluations, energy efficiency, irrigated landscapes, carbon storage and reduction, yield assessments, soil quality, and disease management. This information supports farmers and policymakers in effectively allocating land, implementing crop rotations, and practicing sustainable land management. (Khavarian Nehzak et al., 2022). Remote sensing satellite data serves as an excellent resource for producing up-to-date LULC classifications (Steinhausen et al., 2018), and extensive Earth Observation (EO) datasets are routinely employed to collect information on LULC and land use/land cover changes (LULCC).(Maus et al., 2019). This data can guide policies concerning land zoning, conservation areas, and agricultural planning. Prakashi et al. (2011) proposes various approaches for mapping land use across landscapes. The use of Satellite Image Time Series (SITS) is beneficial for comprehending landscape dynamics, such as deforestation, greenhouse gas emissions, and agricultural expansion. (Petitjean et al., 2012). Despite the advancements in remote sensing technologies, LULC classification remains complex and is influenced by various factors. Recently, there has been significant progress in remote sensing technologies, leading to the release of numerous satellite datasets with differing spectral, temporal, and spatial resolutions for both public and commercial applications. In the last two decades, moderate spatial resolution instruments, such as the Moderate Resolution Imaging Spectroradiometer (MODIS), have been the focal point for algorithms, products, and applications, owing to their increased accessibility and ease of data processing. Moderate-resolution data is often utilized to derive phenological measurements, which help in understanding phenological cycles and identifying subtle differences among similar classes. A review by Chaves et al. (2020) emphasizes the importance of utilizing Landsat-8 and Sentinel-2 data for creating accurate and timely LULC maps. Currently, commercial optical satellites like QuickBird, WorldView, and PlanetScope, which offer higher spatial resolutions, are employed. Notably, PlanetScope imaging provides new research opportunities due to its 3-meter spatial and temporal resolution.

2. **Forest Management:** Remote sensing is instrumental in monitoring forest health, deforestation, and canopy cover. This information is essential for sustainable forest management, conservation efforts, and climate change mitigation policies. Satellites and aircraft equipped with remote sensors can gather data on forest structure, health, and changes over time. The processed and analyzed data is then utilized for various forest management tasks. In certain regions around the world, multispectral satellite data—primarily from Landsat and SPOT 1–5—along with Airborne Laser Scanning (ALS) data, have been pivotal in observing these trends.(Barrett et al., 2016). The areas where remote sensing complies with forest management are:

(a)Monitoring Forest Coverage: Remote sensing technology enables accurate mapping of vegetation across extensive forested regions, allowing for the classification of different forest types, detection of changes in forest cover, and assessment of these changes over time. This technology is instrumental in identifying areas prone to deforestation and monitoring ongoing alterations. Foresters rely on this information to effectively manage biodiversity and combat the effects of deforestation.

(b) Monitoring and Detecting Forest Wildfires: Forest fires pose significant threats to both the environment and the economy. Remote sensing satellites are capable of monitoring these fires and providing real-time alerts. Utilizing thermal and infrared sensors, it becomes possible to detect and manage forest fires quickly and effectively.(Fassnacht et al., 2021).

(c) Forest Carbon Sequestration and Biomass Assessment: Remote sensing technology provides estimates of tree heights, diameters, and volumes, facilitating the assessment of forest resources. This data is essential for calculating carbon stocks, which are crucial for climate change research and carbon sequestration strategies. Puliti et al. (2021) demonstrated that utilizing multispectral satellite data enhanced the estimation of biomass changes. Additionally, Breidenbach et al. (2021) improved carbon stock estimates by integrating Landsat-based forest-loss data with comprehensive airborne laser scanning (ALS) data.

(d) Forest Planning and Maintenance: Remote sensing technology facilitates proactive management of forests, aiding in activities such as replanting, harvesting, and overall maintenance. It allows for early detection of disease outbreaks and pest infestations. Additionally, remote sensing supports the development of strategies aimed at mitigating disasters, pests, and diseases, thereby preserving forest health.

(e) Biodiversity and Ecosystem Maintenance: Understanding the habitat requirements of wildlife and their responses to habitat changes is essential for conserving biodiversity and sustaining functional ecosystems. Remote sensing plays a critical role in assessing wildlife habitats and monitoring the factors that influence their health and stability. (Duncanson et al., 2022).

3. **Phenology Studies and Vegetative Change:** Remote sensing phenology studies leverage satellite sensor data to measure the light wavelengths that are absorbed and reflected by green plants. Plant leaves, rich in pigments, absorb visible light (specifically red light) while reflecting near-infrared light, which is invisible to the human eye. As a plant progresses through its growth cycle, these reflectance characteristics change. The Normalized Difference Vegetation Index (NDVI), derived from sensors such as the Advanced Very High-Resolution Radiometer (AVHRR), is widely employed to monitor vegetation moisture conditions. Various satellite sensors capture reflected red and near-infrared light, which is then processed through algorithms to create vegetation indices. NDVI values range from +1.0 to -1.0, providing insights into vegetation health. This index is particularly useful for monitoring at continental to global scales, as it accounts for variations in illumination, surface slope, and viewing angle. However, NDVI may saturate in areas of dense vegetation and is sensitive to soil color; these limitations can be addressed using the Soil-Adjusted Vegetation Index (SAVI). Over time, average NDVI values help establish “normal” growing conditions, allowing for the analysis of vegetation health, stress, and changes resulting from factors such as deforestation or wildfires during different phenological stages.(Sarmin et al., 2024)

. Literature Review

Current Methods of Biomass and Carbon Stock Estimation

Carbon Sequestration and Biomass Estimation: Carbon sequestration refers to the natural process of capturing CO2 from the atmosphere and storing it in various reservoirs, such as oceans and terrestrial ecosystems. Accurate measurement and reporting of carbon stocks are crucial for participation in carbon trading schemes. However, ground-based biomass measurements can be expensive, which prompts the exploration of more cost-effective remote sensing methods to estimate carbon stocks following farmland revegetation.

Calibrating remote sensing data with in-situ biomass measurements offers a potentially economical way to report carbon stocks across landscapes. This method provides timely data based on direct observations of actual carbon stocks, rather than relying solely on modeled values. High-resolution remotely sensed imagery can be analyzed at the pixel level (pixel-based analysis) or through techniques that extract multi-pixel features (feature extraction or fractional coverage), including the examination of individual canopy crowns, as demonstrated by Bunting and Lucas (2000), provided the images have sufficiently fine spatial resolution.

Although the use of pixel-based vegetation indices (VIs) for estimating biomass is well established—examples include the normalized difference vegetation index (NDVI), enhanced vegetation index (EVI), and ratio vegetation index (RVI) in forests, grasslands, and woodlands—these techniques have rarely been applied to estimate carbon stocks in shrublands. The broader application of remote sensing for calibrating VIs to biomass indicates that the relationship between VIs and biomass can vary based on species, seasonal changes, and the scale of vegetation and pixels.

Analysis of annual fluctuations in cropland carbon stocks reveals dynamic changes over time, influenced by various factors affecting carbon dynamics within agricultural ecosystems. One significant driver of these fluctuations is the adoption of diverse land management practices by farmers. For instance, alterations in tillage methods, crop rotation strategies, and the use of organic amendments can significantly impact carbon sequestration rates in croplands. Practices like conservation tillage and cover cropping are known to enhance soil carbon storage by minimizing soil disturbance and promoting organic matter accumulation.

Climatic variations also play a crucial role in shaping carbon dynamics in croplands. Factors such as temperature, precipitation, and extreme weather events directly affect soil organic matter decomposition rates, plant growth, and carbon input into the soil. Warmer temperatures and shifts in precipitation patterns may accelerate soil carbon decomposition, leading to reduced carbon stocks, particularly in drought-prone or waterlogged regions.

Changes in vegetation cover further contribute to temporal fluctuations in cropland carbon stocks. Variations in crop types, planting densities, and land-use conversions influence biomass production and the subsequent carbon sequestered in agricultural soils. For example, the expansion of croplands into previously uncultivated areas or the conversion of croplands to other uses, such as urbanization or afforestation, can significantly alter carbon storage levels.

Understanding the temporal dynamics of cropland carbon stocks is vital for implementing effective carbon sequestration strategies and sustainable land management practices. By identifying the factors driving these fluctuations, policymakers and land managers can develop targeted interventions to enhance carbon storage in croplands, mitigate the impacts of climate change, and promote agricultural sustainability. Additionally, ongoing monitoring and research are essential for better quantifying and predicting the long-term implications of these temporal changes on ecosystem carbon dynamics and global carbon budgets.

Estimation of Aboveground Biomass: Accurate biomass estimations across all land cover types are necessary for carbon accounting, although reliable estimates in the literature are limited. Biomass and carbon content are typically higher in tropical forests, highlighting their significance in the global carbon cycle. With appropriate conservation and management practices, tropical forests hold significant potential for CO2 mitigation. (Sandra Brown, 1997). The biomass assessment methods outlined here are not limited to forests, agriculture, or pastures; they evaluate current biomass regardless of land cover type. These methods can be applied in areas where trees are predominant, including closed and open forests, savannahs, plantations, gardens, and live fences, as well as in agricultural and pasture systems featuring various crop rotations and combinations of crops, trees, and pastures.

When assessing biomass, it is essential to consider all components of the ecosystem, including the live mass above and below ground of trees, shrubs, palms, saplings, and the herbaceous layer on the forest floor, as well as the inert fraction present in debris and litter. These components represent the majority of the total aboveground biomass in an ecosystem, and their estimation typically does not pose significant logistical challenges.

In this context, biomass is defined as the total amount of live organic matter and inert organic matter (IOM), both aboveground and belowground, expressed in tons of dry matter per unit area (e.g., per individual plant, hectare, region, or country). Biomass density is commonly measured in terms of mass per unit area, such as tons per hectare. To determine the total biomass for a region or country, one can upscale or aggregate the biomass density measurements from the minimum area surveyed.

Remote Sensing for Aboveground Biomass Estimation: Remotely sensed data refers to information collected by sensors located on platforms that do not directly touch or are in close proximity to the biomass being measured. This data includes images captured from both aircraft and satellites. Remote sensing imagery is particularly valuable when validated or verified against ground measurements and observations (often referred to as "ground truth").

Remote sensing can facilitate aboveground biomass estimation in at least three ways:

1. **Classification of Vegetation Cover:** This approach generates a vegetation type map, partitioning the spatial variability of vegetation into relatively uniform zones or classes. Such classification aids in identifying species groups and allows for spatial interpolation and extrapolation of biomass estimates.

2. **Indirect Estimation of Biomass:** This method employs quantitative relationships (e.g., regression equations) between band ratio indices (like NDVI, EVI) or other metrics, such as direct radiance values or digital numbers per pixel, and direct biomass measurements or related parameters, such as leaf area index (LAI).

3. **Sampling Framework for Ground Observations:** By partitioning vegetation cover into uniform zones or classes, remote sensing can serve as a sampling framework for locating ground observations and measurements.

Using band ratio indices, such as NDVI and EVI, requires detailed measurements of additional morphological and physiognomic parameters of the vegetation canopy, such as LAI. There must also be a strong relationship between LAI and both NDVI and biomass. The strength and form of these relationships can vary significantly based on canopy type and structure, vegetation health, and various environmental parameters. Much of the literature discussing these relationships remains an area of ongoing research. ((Baret et al., 1989); (Wiegand et al., 1991); (Daughtry et al., 1992); (Gupta et al., 2000)).

Remote-sensing products serve as a valuable framework for upscaling detailed site measurements of aboveground biomass. However, their effectiveness is contingent upon the strength of the relationships identified for specific geographic areas.

The classification of vegetation cover using multispectral satellite imagery follows well-documented procedures, techniques, and algorithms in the remote sensing literature, which are beyond the scope of this report. In summary, the steps involved include:

1. **Multispectral Image Acquisition:** Typically involves capturing images using Landsat Thematic Mapper (TM) bands 1, 2, 3, 4, 5, and 7, followed by image enhancement techniques such as stretching and filtering.

2. **Corrections and Georeferencing:** This includes geometric and radiometric corrections, as well as georeferencing (registration) to ensure spatial accuracy.

3. **Creation of False Color Composite (FCC) Images:** Usually constructed using TM3 (red), TM4 (short-wave infrared), and TM5 (near-infrared) bands.

4. **Selection and Sampling of Training Sites:** Identifying locations on the image where the vegetation cover type has been observed, recorded, and validated. The clustering of pixels from these training sites in feature space is then analyzed.

5. **Supervised Classification:** This step involves using reflectance values from the training sites and the classes assigned to them to extend the classification to the rest of the FCC image through chosen classificatory algorithms.

6. **Raster-to-Vector Conversion (Optional):** This additional step converts the resulting classified image (in raster format) to vector format, creating a polygon map of vegetation classes.

The accuracy of the resulting vegetation map depends on several factors: the complexity of the species mix within the crop, vegetation, or forest cover; the spatial variability of the cover in the area; the selection of representative training sites; and the appropriateness of the chosen classification algorithm based on the nature of the clusters formed by the training sites and the histograms of radiance values for each image band used in the classification.

The generated vegetation map should effectively illustrate the spatial variability of the primary vegetation or forest cover classes in the area of interest, represented either in raster/grid-cell format or as polygons in vector format. Figure 1 depicts the methodological framework for estimating aboveground biomass.

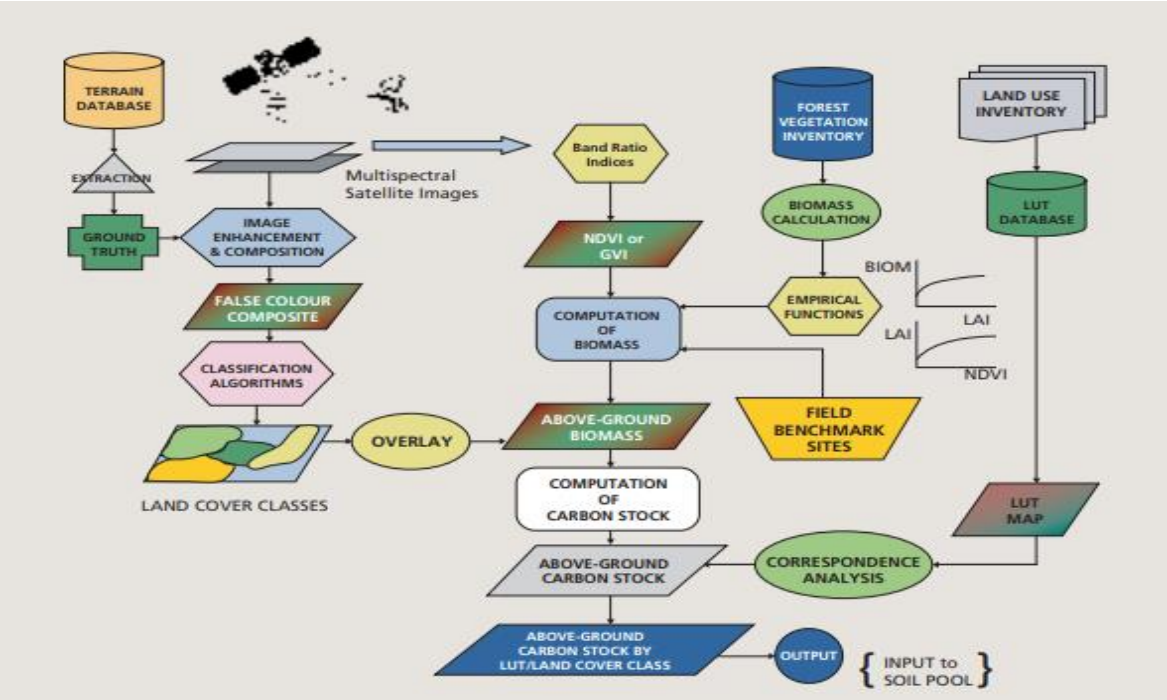

Figure 1 Estimation of biomass and carbon in aboveground pool

Classification and Mapping of Vegetation Cover through Air-Photograph Interpretation

Techniques for classifying and mapping vegetation cover via air-photograph interpretation were developed prior to the analysis and interpretation of satellite images. These techniques have long been standard practices in identifying vegetation classes and forest stands, playing a critical role in conventional land cover mapping and forest inventory work in many countries. Therefore, this report does not delve deeply into these methods.

Air-photograph interpretation, when combined with field sampling and validation, utilizes various photographic characteristics—such as photo patterns, texture, tone, and stereoscopic vision—along with tools like the parallax bar to delineate classes of crops, vegetation cover, or forest stands. The boundaries of these classes are then transferred to a map, creating mapping units that can be digitized into a Geographic Information System (GIS), resulting in vector polygons.

The process of generating a land cover class map from multispectral satellite images typically involves multiple steps:

1. **Landsat TM Images**: Utilizing different bands to gather data.
2. **Air Photos**: Incorporating aerial photographs to enhance interpretation.
3. **Vegetation Raster Map**: Creating an initial vegetation map from satellite data.
4. **Unsupervised Classification**: Automatically grouping pixels based on their spectral characteristics.
5. **Supervised Classification**: Employing training sites to guide the classification process.
6. **Photo Interpretation**: Analyzing aerial images for detailed classification.
7. **False Color Composite Raster Map**: Generating a visual representation of the data for easier analysis.
8. **Pre-processed Images**: Ensuring that the images are corrected for any distortions.

The end result of these procedures is comparable to the outcomes achieved through the interpretation and classification of satellite images. The accuracy of either method can vary based on the expertise of the photo interpreter, the density of field samples used for validation, and how representative those samples are of the variability in vegetation classes.

Both multispectral satellite image interpretation and air-photo interpretation ultimately contribute indirectly to estimating aboveground biomass. The literature presents a variety of methodologies within this domain, ranging from conventional forest inventories based on ground measurements of individual tree dimensions (allometric measurements) to the utilization of yield tables, regression equations, and measurements obtained from various sensor platforms.(Foody et al., 1996).

A commonality across all estimation techniques is the necessity for validation through ground measurements of tree geometries and volumes. In this report, remote-sensing and ground-based methods are treated as complementary components of a unified procedure. This integrated approach allows for the use of remote-sensing techniques alongside spatial interpolation and extrapolation methods to effectively

upscale and downscale estimates across different areas. Furthermore, these techniques provide a valuable spatial framework for field sampling.

Given the practical and logistical challenges related to the availability and cost of remote-sensing materials in developing regions, this report emphasizes the importance of obtaining ground measurements. These measurements form the foundation for validating all estimation procedures, including those utilizing remote sensing.

Multipurpose Field Surveys and Sampling Design

The sampling design for collecting aboveground biomass data should be multipurpose to enhance data collection efficiency and minimize costs. The sites selected for aboveground biomass measurements should also facilitate assessments of biodiversity and land degradation by observing relevant indicators.

The multipurpose nature of the sampling design requires that it yields data for the following:

1. **Aboveground Biomass Estimation:** This includes morphometric measurements of standing vegetation, encompassing stem and canopy dimensions of various strata of trees and shrubs, along with debris, deadwood, saplings, and samples of herbs and litter fall.
2. **Biodiversity Assessment:** Identification and quantification of plant species for calculating plant diversity indices.
3. **Land Degradation Assessment:** Site measurements and observations of key indicators that reflect the status of land degradation.

For this purpose, sampling quadrats of regular shapes—specifically 10 x 10 m, 5 x 5 m, and 1 x 1 m—are employed and nested within one another to measure biomass, biodiversity, and land degradation across the landscape. The dimensions of these quadrats align with recommended practices in ecological literature and represent a balanced compromise among accuracy, practicality, and efficiency in terms of time and effort. Figure 2 illustrates the nesting arrangement of the quadrats.

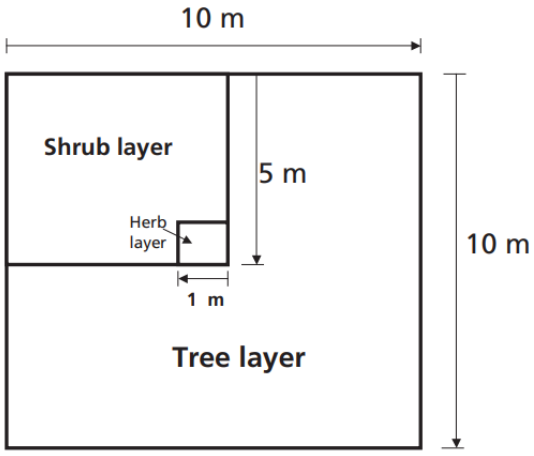

Figure 2 Quadrat sampling for biomass

The selection of sample sites and their locations is carried out through a series of activities aimed at achieving a highly representative sample size and distribution, all while minimizing costs. This process is inherently complex due to the different spatial scales of variability for each variable of interest, including plant biodiversity, the spatial variability of aboveground biomass, and the status of land degradation in the studied area.

The sampling flowchart illustrates the systematic approach employed in this study. Whether the vegetation or land cover classes are derived from multispectral satellite image interpretation or air photo analysis, they are transformed into raster or vector maps that serve as the foundation for stratification. This stratification facilitates the allocation of sampling sites to various land cover classes, referred to as strata in this context. A stratified random sampling design is employed, where the probability of selecting sampling sites is proportional to the area covered by each land cover class (stratum).

Each stratum is characterized by specific land cover or vegetation types, with tools for defining these strata including the classification of satellite imagery, photointerpretation of aerial photographs, and preliminary ground observations and measurements (i.e., the establishment of training sites) to verify the accuracy of the classifications.

Defining the variables to be observed or measured is a critical component of the survey design. These variables are categorized into three groups:

1. **Abiotic Factors**: These include site characteristics such as elevation, slope, aspect, local physiography, soil type, and types of disturbances present.
2. **Biotic Factors**: This category encompasses aspects of terrestrial flora relevant to biomass measurement and biodiversity. Key considerations include vegetation type, successional state, the number of species across different layers, and the number of individuals for each species within these layers.
3. **Land Degradation Factors**: These include relevant indicators that assess physical, chemical, and biological land degradation.

Field data forms are developed and printed for each of the three areas of concern related to field sampling: aboveground biomass (morphometric measurements), biodiversity indices, and land degradation indicators. These field forms contain designated spaces for recording data on the relevant variables associated with each of the three focal areas. Chapter 6 provides examples of these field data forms.

Furthermore, morphometric measurements and plant diversity are assessed across two distinct landscape element types (strata). It is essential to ensure that dissimilarities within the same strata (polygons) are significantly lower than those between different strata. The following statistical model illustrates how variability can be partitioned into various sources and should be utilized for hypothesis testing during data processing, employing a one-factor analysis of variance (ANOVA) design. Additionally, normality and homogeneity of variance should also be assessed:

$$Y_{ij} = \mu + \vartheta t_i + \varepsilon_{ij}$$

where, for example in the case of biodiversity indices: Y_{ij} is number of species or abundance in the j_{th} forest stand within the i-th type of vegetation (stratum); μ is the general mean of all strata; ϑt_i is the effect of i_{th} vegetation type on morphometric or plant diversity measurements; and ε_{ij} is the error in the j_{th} stand within the i_{th} type of vegetation (stratum). The target accuracy for the sampling design should be set at 95% reliability with a 5% margin of error in the estimations. The sample size must be determined for each stratum; however, prior information about the variance of the variables to be studied (e.g., morphometric measurements, number of species, and abundance) is typically lacking. To address this, two steps are recommended to obtain field information:

1. **Pre-Survey Estimation of Prior Variance**: This step involves a subjective assessment of the pre-survey sample size.
2. **Calculation of Sample Size for Each Stratum**: The sample size is calculated using the prior variance obtained from the pre-survey, applying standard statistical formulas based on the variance of the variable of interest. For variables such as the total number of plant species, it is important to compile and compute "saturation curves" of species versus the number of sampling quadrats. This helps establish the total number of quadrats required to adequately represent the variability of plant species populations. The assessment team should strive to attain such curves unless constrained by strong economic or logistical challenges.

Sampling sites (quadrats) are located in the field by randomly selecting coordinate pairs for each site using a random number generator, once the number of sampling sites for each stratum or vegetation/land cover class has been determined. The number of samples for each stratum is selected in proportion to its extent, utilizing the vegetation map. The coordinate pairs of each site are then located in the field using a global positioning system (GPS).

It is possible to encounter multiple strata of trees within each vegetation type, especially in tropical areas. This variability can be documented by recording the number of canopy layers present at each 10 x 10 m quadrat. For all trees within each layer defined by either height or successional stage, the number of plants by species should be recorded. For instance, in a tropical forest with three observed canopy layers, the categorization could be as follows:

- **First Layer**: Trees 20 m and higher
- **Second Layer**: Trees between 10 m and 20 m
- **Third Layer**: Trees less than 10 m

One of the challenges in practical fieldwork is species identification. Due to logistical constraints, it may not be feasible to collect plants with all necessary morphological components for herbarium identification. Therefore, local knowledge from individuals who have lived and worked in or near the forest can be invaluable. Local people often possess the ability to accurately identify species using local or botanical names, providing an effective alternative to employing a full-time botanist within the multidisciplinary team. However, validation procedures should be established to ensure the accuracy of species identification methods by collecting samples for botanical identification in a herbarium whenever possible.

Data collection should be organized and systematic. A digital database system can be designed prior to fieldwork and modified as needed to accommodate real-time field conditions. This facilitates data entry into databases that can be linked to data processing software, computer modeling, and GIS applications. A commercially available database management system (DBMS) can serve this purpose, customized to reflect the specific information needs of the project. Common DBMS software packages can be utilized for storing and later processing field data.

Calculation of Aboveground Biomass from Allometric Methods

Aboveground biomass is estimated from field measurements taken at specific sites (quadrats) where the landscape has been sampled. The procedural steps for calculating aboveground biomass from such field data are outlined as follows:

To compute aboveground biomass in a watershed, the focus is primarily on forest layers. For methodological clarity, biomass calculations for trees and shrubs are divided into two categories based on tree morphology:

1. **Calculation of Biomass for Trunk or Stem**
2. **Calculation of Biomass for Canopy or Crown**

This distinction is necessary as different procedures and approaches are employed for estimating biomass in each case.

In each 10 x 10 m quadrat, the following allometric measurements are collected from field sampling of each tree within the quadrat boundaries (refer to Figure 3):

- Tree height (H)
- Diameter at breast height (DBH)
- Diameter of the canopy or crown in two perpendicular directions, referred to here as “length” (L) and “width” (W)
- Height to the base of the crown (Hc)
- Percentage of foliage cover in the crown or canopy (Fc)

Two approaches can be used to calculate trunk and canopy biomass, depending on the conditions and tools available during data collection, as well as the required degree of accuracy:

1. **Allometric Method**
2. **Linear Regression Equations Method**

For the allometric method, the basal area (A_b) of the trunk must first be considered. If this measurement has been recorded using conventional forest inventory equipment, the subsequent section can be disregarded. However, if the basal area has not been measured in the field, it can be estimated using the following formula:

$$A_b = \Pi * r^2$$

where: $\prod$ = 3.1415927.

and r is the radius of the tree at breast height (0.5 DBH).

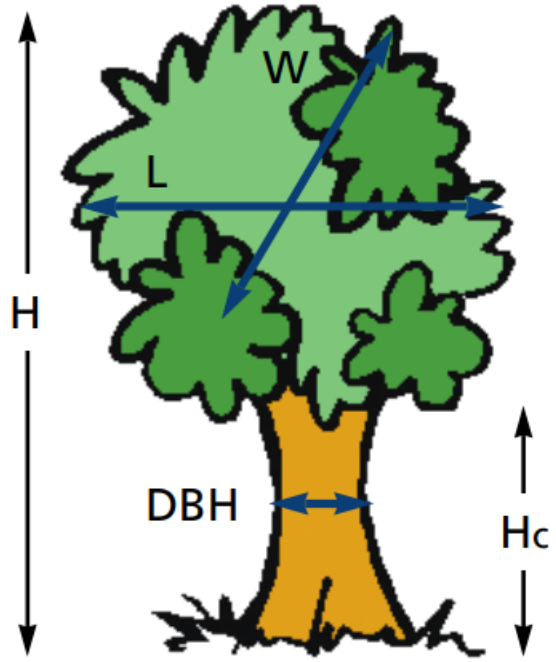

Figure 3 Allometric measurements in forest

With A_b, the volume (V) in cubic metres can be calculated from:

$$V = A_b * H * K_c$$

where: A_b is the basal area; H is the height; and K_c is a site-dependent constant in standard cubing practice used in forest inventory (e.g. in Texcoco, Kc = 0.5463).

Using the calculated volume of the trunk, total trunk biomass in kilograms may be calculated by multiplying by the wood density (WD) corresponding to each tree species measured:

$$\text{Biomass} = \text{V x WD x 1 000}$$

The linear regression equation approach involves selecting a regression equation that best fits the conditions of the study area. Linear regression models have been applied to data across various sites and ecological conditions globally. The work done by (Brown et al., 1989) and (Sandra Brown, 1997) on estimation of biomass of tropical forests using regression equations of biomass as a function of DBH is central to the use of this approach. Some of the equations reported by (Brown et al., 1989) have become standard practice because of their wide applicability. Using any of these methods, tree biomass can be estimated by applying the corresponding regression equation. Plots illustrating tree biomass estimates by diameter at breast height (DBH) using various regression equations for different cover types can demonstrate the variations in predictions.

When only the trunk biomass has been estimated (e.g., through allometric calculations), the biomass of the crown (canopy) must also be estimated and added to the trunk biomass. The first step in this process is to estimate the volume occupied by the canopy. Given the variability in tree crown shapes across species and even among individual trees of the same species, some generalizations must be made regarding canopy density and the distribution of branches and foliage.

The methods used for estimating crown volume provide reasonable approximations under current practical conditions. The crown or canopy volume can be estimated using a function based on the geometric properties of the crown shape. The volume estimated by the equations in Figure 4 represents the gross total volume.

Approximate shape of the crown	Equation
Conical	$V\ (m^3) = \pi \times \frac{Db^2 \times Hc}{12}$
Parabolic	$V\ (m^3) = \pi \times \frac{Db^2 \times Hc}{8}$
Hemispherical	$V\ (m^3) = \pi \times \frac{Db^2}{12}$

Figure 4 Estimation of crown or canopy volume as a function of the shape of the crown

In reality, much of the crown volume consists of empty space. To estimate the actual proportion of the volume occupied by branches and foliage, one can stand beneath the canopy, next to the trunk, and make a careful visual assessment of the canopy structure. This proportion is then used to adjust the crown volume by discounting the air space.

$$solid\ volume\ =\ V(m^3)\ x\ proportion\ of\ branches\ and\ foliage\ in\ crown\ volume.$$

Where possible, samples of branches and foliage should be collected and taken to the laboratory to determine wood density (WD) and dry matter content in the foliage. This ensures a more accurate approximation of biomass, leaving only the estimation of foliage density as a somewhat subjective element in the process. Literature on calculating the WD of the crown is limited. For the methodology presented here, a conservative approach is adopted: if the WD value of the tree is known, it is divided in half to estimate the density of leaves and small branches in the crown. If the WD is unknown, then half the average WD value for species found in the quadrat plot or within the same mapping unit or land cover polygon is applied.

Total biomass is calculated for each tree in the sample quadrat by adding the trunk and crown biomass estimates, then summing the results for all trees in the sample quadrat. This value can then be converted to tones per hectare. To the biomass estimate from the 10 x 10 m quadrat, the estimates from shrubs, deadwood, and debris measured in the nested 5 x 5 m quadrat need to be included. Shrub volume is estimated similarly to that of tree trunks by calculating the volume of the stem. However, considerable reductions in wood density are applied due to the higher moisture content in the green tissue of shrubs.

Additionally, the contribution of foliage to the volume of shrubs is considered negligible and, therefore, is not included in the overall estimation of total biomass.

The herbaceous layer, litter, and other organic debris collected from the 1 x 1 m quadrat are taken to the laboratory, dried, and weighed. The resulting value provides the dry organic matter estimate per square meter. This biomass calculation is then extrapolated to the 100 square meters of the largest quadrat. This final figure can be added to the estimates of trunk and crown biomass calculated earlier, yielding a total aboveground biomass value for each of the field sampling sites (10 x 10 m quadrats).

Given the significance of aboveground biomass for carbon accounting and its use in modeling soil carbon dynamics (SOC), certain minimum data sets should be gathered during field surveys. Additionally, specific information about the tree species is required to complete the data sets, including:

- Wood density
- Volumetric coefficient
- A method to readily calculate the density of wood plus foliage of the canopy with minimal field data

These variables constitute the minimum data set for biomass estimation. They are easily obtainable and can be measured at a low cost.(Ponce-Hernandez, 2004)

Vegetation Indices in Carbon Stock Assessment

Vegetation indices such as the Normalized Difference Vegetation Index (NDVI) and the Enhanced Vegetation Index (EVI) are widely used to estimate vegetation biomass and carbon stocks. NDVI is particularly effective for detecting the presence and health of vegetation, while EVI enhances sensitivity to areas with high biomass. However, the effectiveness of these indices can vary based on vegetation type, seasonality, and environmental conditions. To achieve more accurate assessments, calibration with ground-based measurements is often necessary.(Pan et al., n.d.)

Remote sensing technology has become instrumental in analyzing spatio-temporal patterns of vegetation phenology, enabling researchers to assess vegetation health and productivity on a pixel-by-pixel basis. The Normalized Difference Vegetation Index (NDVI) is the most widely used measure of photosynthetic activity in vegetation and serves as a foundational metric for deriving phenological parameters. (Miura et al., 2001). Historically, NDVI data were collected using NOAA-AVHRR instruments. More recent advancements include the use of Aqua/Terra MODIS and SPOT sensors, which provide higher spatial resolution and improved preprocessing capabilities for vegetation analysis.(Pan et al., n.d.).

Despite the advantages of remote sensing, current NDVI data are often limited to coarse and medium spatial resolutions (ranging from 250 to 8000 meters). This limitation can hinder the detection of small-scale disturbances, such as agricultural activities. (Begue et al., 2014).

Some researchers have utilized Landsat TM-like multi-temporal images for land cover change mapping. However, the infrequent availability of these images often does not meet the demand for high temporal resolution, particularly during critical growth periods. To address this challenge, data fusion technologies have been proposed to combine the strengths of different satellite datasets, enabling the generation of simulated high spatio-temporal resolution imagery.(Pan et al., n.d.)

Challenges in Biomass Estimation Using Remote Sensing

Despite advancements in remote sensing, several challenges persist in accurately estimating biomass and carbon stocks. These challenges include the complexity of vegetation structure, seasonal variations, cloud cover, and the differing spatial resolutions of satellite imagery. Furthermore, the relationship between vegetation indices and biomass is not always linear, necessitating additional calibration and validation through ground-truthing techniques.

Methodology

Satellite Image Processing

In this study, we processed satellite imagery from Sentinel-2, Landsat 8, and Landsat 9 to derive vegetation indices and classify land cover types within the specified study area. Our primary focus was on generating and analyzing time-series data using the Normalized Difference Vegetation Index (NDVI) and the Enhanced Vegetation Index (EVI) for the year 2023.

Geometry

Figure 5 area of study

Turin, Italy

Turin, located at 45.0703° N latitude and 7.6869° E longitude, is situated in the northwestern part of Italy, within the Piedmont region. The city is positioned at an elevation of approximately 240 meters above sea level and is nestled between the foothills of the Alps to the west and the fertile Po River Valley, contributing to its rich geographic diversity.

Climate and Environmental Conditions:

- **Mean Annual Temperature:** The average annual temperature in Turin is 13.5°C. Winters are cold, with January temperatures averaging around 2°C, while summers can be warm, with July averaging around 25°C.
- **Mean Annual Precipitation:** The region experiences an average annual precipitation of about 950 mm, with spring and autumn typically being the wettest seasons. Rainfall is generally well-distributed, though occasional storms and summer thunderstorms are common.
- **Humidity:** Turin has moderate humidity levels, typically ranging between 60% and 80% throughout the year, which contributes to the region's diverse agricultural practices.

Agriculture and Industry:

The surrounding plains of Turin are highly fertile, supporting intensive agriculture, including the cultivation of cereals, vineyards, and fruit orchards. Common crops in the area include wheat, corn, and rice, while the vineyards produce world-renowned wines like Barolo and Barbaresco.

In addition to agriculture, the region is a key industrial hub, known for its automotive industry (home to Fiat), as well as advanced manufacturing and technology sectors.

This blend of urban development, industrial activity, and agricultural production, coupled with natural ecosystems, makes Turin a significant area for studying carbon sequestration and environmental monitoring. The seasonal variations, elevation, and agricultural practices all impact vegetation dynamics, making it an ideal location for remote sensing studies focused on biomass and carbon stock estimation.(*Regional Innovation in Piedmont, Italy*, 2021)

Dataset

Sentinel-2:

- After 2022-01-25, Sentinel-2 scenes with PROCESSING_BASELINE '04.00' or above have their DN (value) range shifted by 1000. The HARMONIZED collection shifts data in newer scenes to be in the same range as in older scenes.

  Sentinel-2 is a wide-swath, high-resolution, multi-spectral imaging mission supporting Copernicus Land Monitoring studies, including the monitoring of vegetation, soil and water cover, as well as observation of inland waterways and coastal areas.

  The Sentinel-2 data contain 13 UINT16 spectral bands representing TOA reflectance scaled by 10000Sentinel-2 imagery was filtered based on the date range from January 1, 2023, to December 31, 2023. The filtering criteria included the removal of images with cloud coverage exceeding 10%.

- Selected images were processed to retain only relevant bands: Blue (B2), Green (B3), Red (B4), Near Infrared (B8), Shortwave Infrared 1 (B11), and Shortwave Infrared 2 (B12).

These bands were scaled using a factor of 0.0001 to convert the reflectance values to the appropriate range.

- Vegetation indices were computed using the scaled bands.
- EVI was calculated using the NIR (B8), Red (B4), and Blue (B2) .

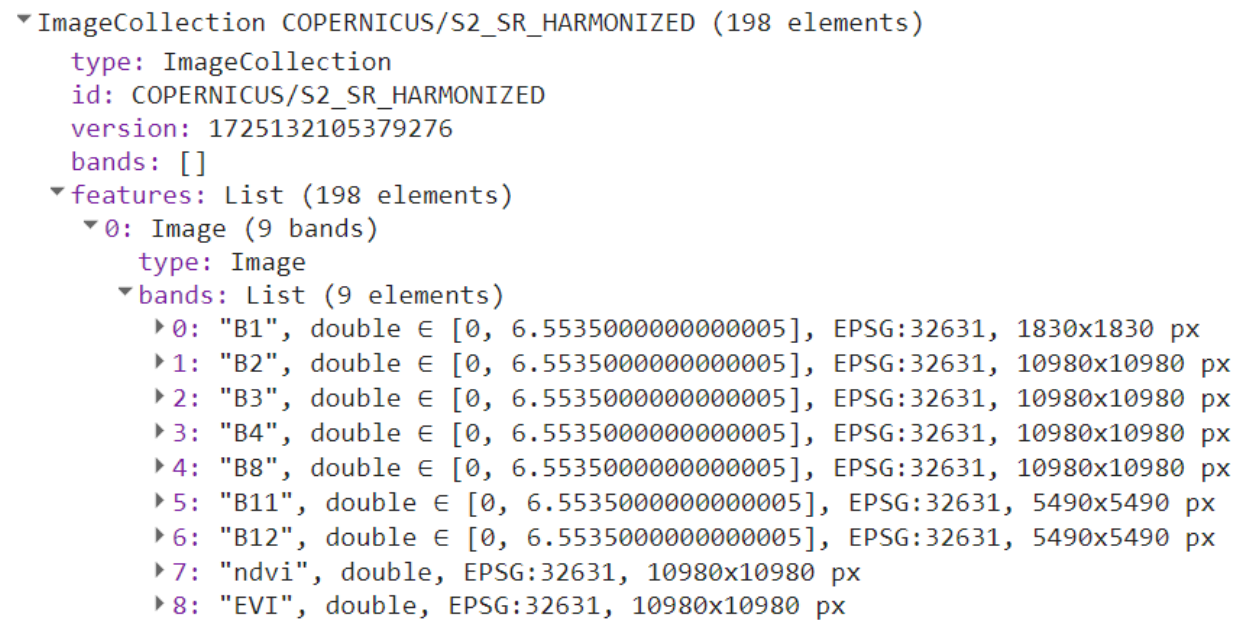

Figure 6 preprocessing of Sentinel 2 images

Landsat 8 and Landsat 9:

- Landsat 8 and 9 Collection 2 Tier 1 calibrated top-of-atmosphere (TOA) reflectance. Calibration coefficients are extracted from the image metadata.

- Landsat scenes with the highest available data quality are placed into Tier 1 and are considered suitable for time-series processing analysis. Tier 1 includes Level-1 Precision Terrain (L1TP) processed data that have well-characterized radiometry and are inter-calibrated across the different Landsat sensors. The georegistration of Tier 1 scenes will be consistent and within prescribed tolerances [<=12 m root mean square error (RMSE)]. All Tier 1 Landsat data can be considered consistent and inter-calibrated (regardless of sensor) across the full collection.

- The T1_RT collection contains both Tier 1 and Real-Time (RT) assets. Newly-acquired Landsat 7 ETM+ and Landsat 8 OLI/TIRS data are processed upon downlink but use predicted ephemeris, initial bumper mode parameters, or initial TIRS line of sight model parameters. The data is placed in the Real-Time tier and made available for immediate download. Once the data have been

reprocessed with definitive ephemeris, updated bumper mode parameters and refined TIRS parameters, the products are transitioned to either Tier 1 or Tier 2 and removed from the Real-Time tier. The transition delay from Real-Time to Tier 1 or Tier 2 is between 14 and 26 days.

- For Landsat 8 and Landsat 9, the imagery was filtered to include data from the same date range and with cloud coverage less than 10%.
- The relevant bands for Landsat 8 (B1, B2, B3, B4, B5, B6, B7) and Landsat 9 (B1, B2, B3, B4, B5, B6, B7) were scaled to reflectance values using a factor of 0.0000275 and an offset of -0.2.
- NDVI and EVI were computed similarly to Sentinel-2 using the scaled bands, with appropriate adjustments for the specific band names and scaling factors of Landsat 8 and Landsat 9.

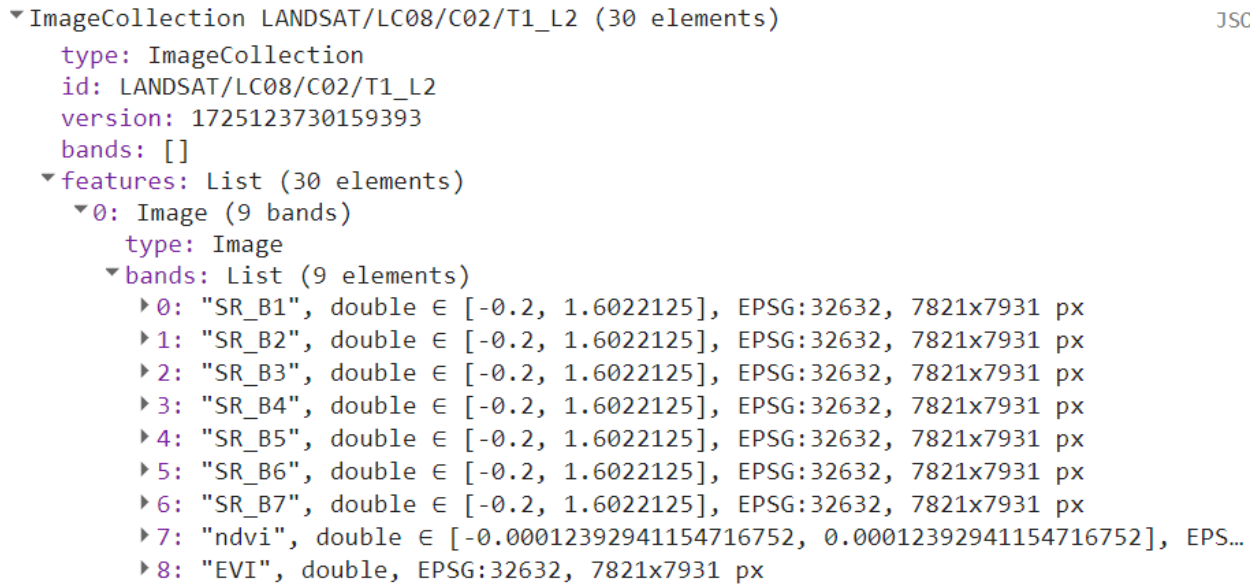

Figure 7 preprocessing of Landsat images

Using NDVI and EVI

Vegetation phenology refers to the timing of seasonal plant growth stages, including leaf development, flowering, senescence, and dormancy (Rathcke and Lacey, 1985). Research on vegetation phenology provides vital insights at multiple levels.

Environmental Level: Vegetation phenology serves as an indicator of climate variability and illustrates how climate influences plant behavior. The seasonal timing and duration of phenological events also govern local carbon uptake, water balance, and surface albedo (Fitchett et al., 2015).

Societal Level: Information about crop phenology can inform decisions related to land use management, nutrient application, and water distribution (Imeson and Prinsen, 2004; Chen et al., 2007).

In regions like East Africa, characterized by a succession of variable rainfall and dry spells, understanding phenological patterns of crops within and between growing seasons is crucial for developing adaptive strategies for climate change resilience. Given the region's strong dependence on agriculture for subsistence, capturing these patterns becomes an essential component of effective climate adaptation.

Precipitation and temperature are primary drivers of the growing season's development, influencing its onset and dormancy (Badeck et al., 2004; Reyer et al., 2013). East African cropping systems are characterized by a rapid response to rainfall events and local dry spells (Cheng et al., 2020). Abrupt variations in these parameters can lead to shifts in planting patterns, ultimately affecting the duration, timing, and yields of the growing season.

From a remote sensing perspective, obtaining a dense series of cloud-free images is essential for accurately depicting local phenology. Satellite remote sensing serves as an effective data source for monitoring phenological changes by measuring leaf reflectance (White et al., 2005; Zeng et al., 2020). Spectral responses in the near-infrared and visible red spectra can be used to calculate the Normalized Difference Vegetation Index (NDVI), a widely utilized proxy for vegetation greenness.

NDVI can effectively track the rapid increases and decreases in surface greenness associated with the onset and conclusion of plant growing seasons (Pettorelli et al., 2005; Zhang et al., 2013). The maximum NDVI value serves as an indicator of the intensity of the peak vegetative stage. Together, the start, end, and duration of the growing season, along with the maximum greenness, constitute the fundamental phenological metrics needed to understand the temporal development of cropping systems throughout the growing season (Reed et al., 1994; Zeng et al., 2020).(Liepa et al., 2024)

In this analysis, the Normalized Difference Vegetation Index (NDVI) and the Enhanced Vegetation Index (EVI) were utilized to monitor vegetation health and land cover changes. NDVI is a widely used vegetation index sensitive to chlorophyll content in plants, making it particularly effective for assessing vegetation density and overall health. In contrast, EVI is specifically designed to enhance the signal-to-noise ratio and reduce atmospheric influences, especially in areas with dense vegetation. The combination of these indices offers a more comprehensive understanding of vegetation dynamics and facilitates accurate land cover classification.

$$\mathrm{NDVI} = \frac{\mathrm{NIR} - \mathrm{Red}}{\mathrm{NIR} + \mathrm{Red}}$$

$$\mathrm{EVI} = 2.5 \times \frac{(\mathrm{NIR} - \mathrm{Red})}{(\mathrm{NIR} + 6 \times \mathrm{Red} - 7.5 \times \mathrm{Blue} + 1)}$$

Computation of Monthly Time Series

To analyze temporal changes, monthly time series data were computed for both NDVI and EVI. The following steps were followed:

Creation of Monthly Composite Images:

- The image collections for NDVI and EVI were filtered to select images from each month of the year.
- For each month, a median composite was generated to reduce the influence of outliers and provide a representative measure of vegetation conditions.

Generation of Monthly Time Series:

- The median images for each month were compiled into time series datasets. These datasets were created for both NDVI and EVI, covering the full year of 2023.
- The time series data were visualized to analyze seasonal patterns and variations in vegetation indices.

Validation Through Time Series

Validation was conducted by comparing the NDVI and EVI data across various times of the year, with particular emphasis on April and October, representing typical spring and autumn conditions.

Comparison of April and October NDVI:

- NDVI and EVI composites for April and October were calculated to evaluate seasonal variations in vegetation health.
- Thresholding was applied to classify different land cover types based on NDVI and EVI values. Considering Figures 9 and 10, which illustrate the annual variation of NDVI and EVI, it is evident that the values for trees and grassland are similar; however, NDVI and EVI values for grassland are lower than those for trees. Upon closer examination of the plots, it is observed that the blue and yellow lines, representing croplands, drop suddenly during the harvesting season. Notably, the trend in EVI is more gradual than that of NDVI. The increase in October can be attributed to the yellow line representing a late-season crop. It is essential to validate this data with additional sources.

- Using Copernicus CORINE Land Cover data on Google Earth Engine, it was confirmed that these points belong to the following classes:

	Point	Palette Class	Landcover Class
1	Point 1	FFFFA8	Agricultural areas; arable land; non-irrigated arable land
2	Point 2	80FF00	Forest and semi natural areas; forests; broad-leaved forest
3	Point 3	FFE64D	Agricultural areas; Heterogeneous agricultural areas; Complex cultivation patterns
4	Point 4	CCF24D	Forest and semi natural areas; Scrub and/or herbaceous vegetation associations; Natural grasslands

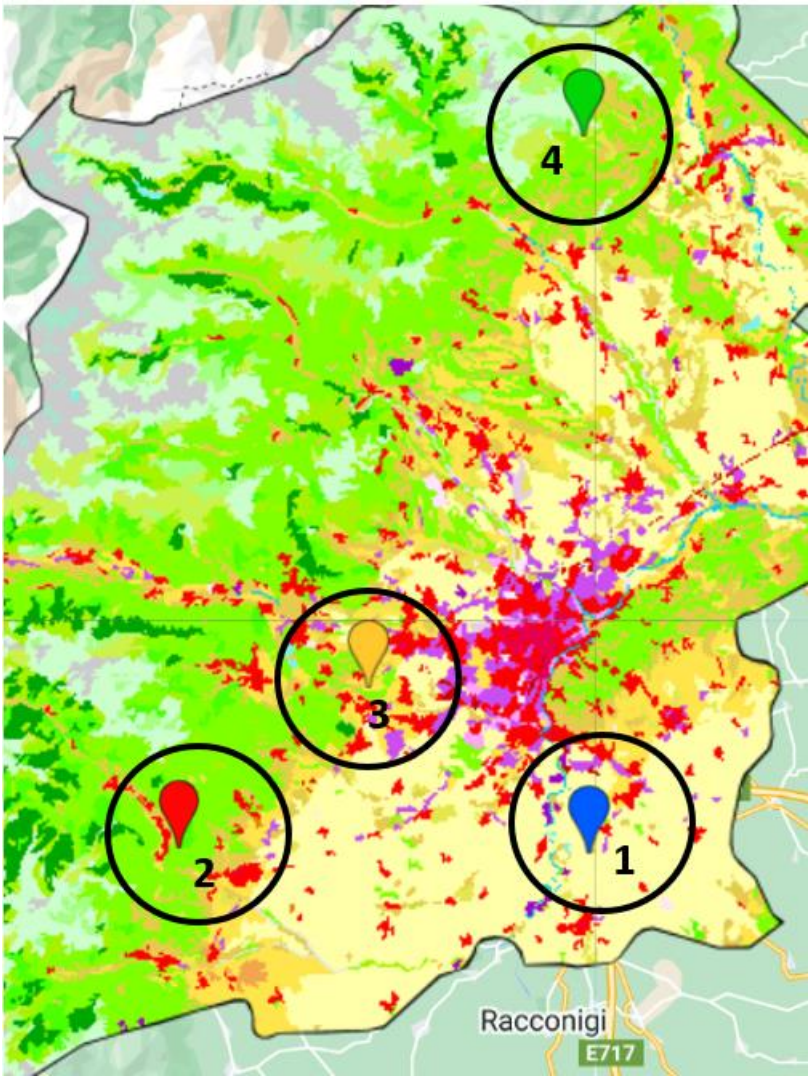

Figure 8 landcover map

Area Calculation and Analysis:

- The areas of different land cover types were calculated based on the classified NDVI images for April and October. This was accomplished by multiplying the binary classification images by pixel area and summing the results to obtain total areas in hectares.

Time Series Charts:

- Time series charts for NDVI and EVI were generated to analyze temporal changes and validate the accuracy of the classifications. These charts offered insights into vegetation trends over time and facilitated the interpretation of seasonal and annual variations. This detailed approach ensured a robust analysis of vegetation dynamics and land cover classification, leveraging the strengths of NDVI and EVI for accurate and meaningful results.

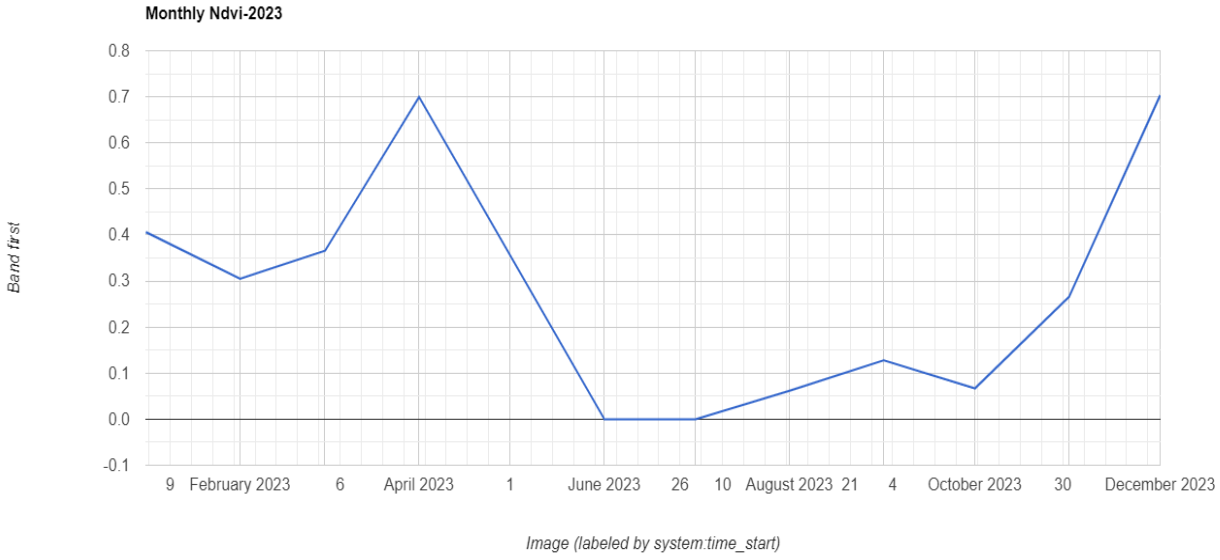

Figure 9 Monthly NDVI 2023

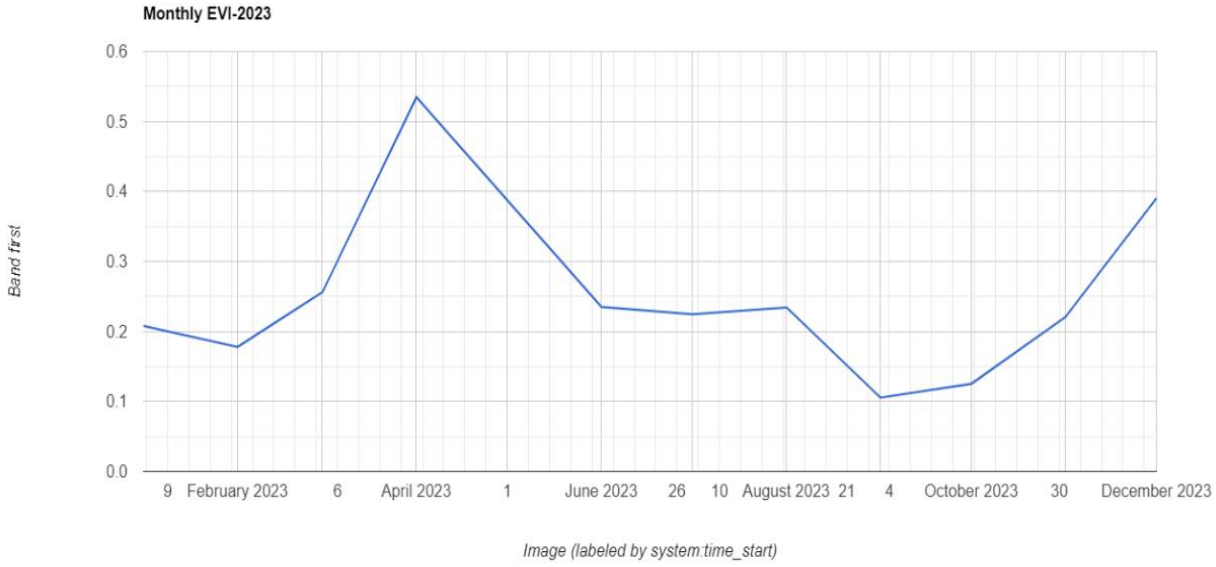

Figure 10 Monthly EVI 2023

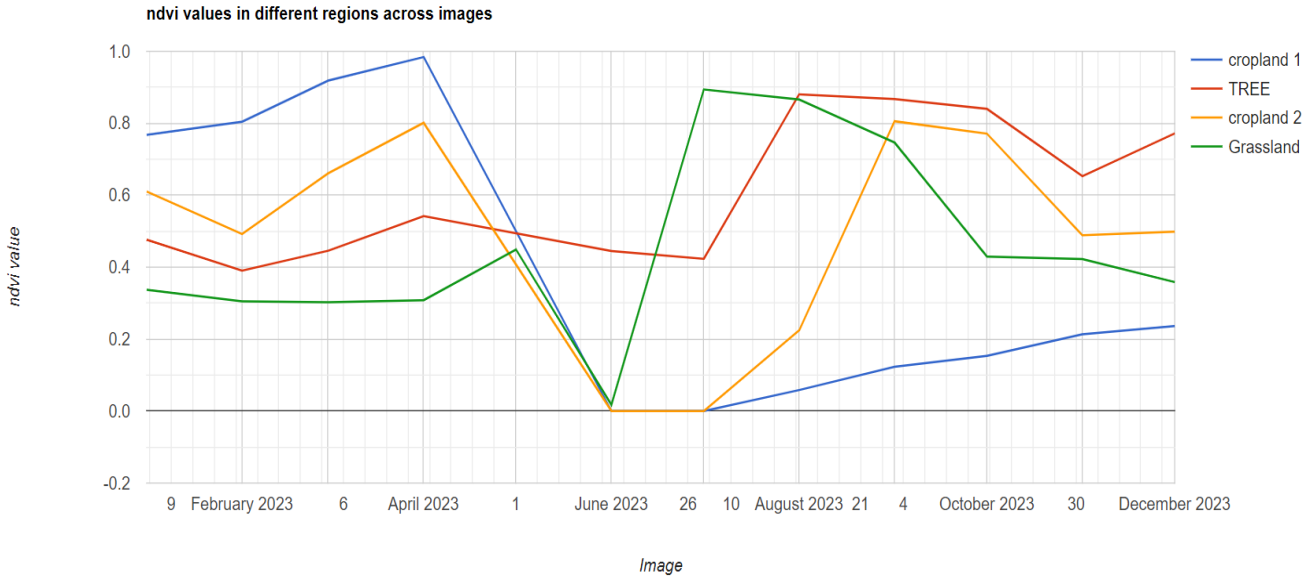

Figure 11 NDVI region timeseries

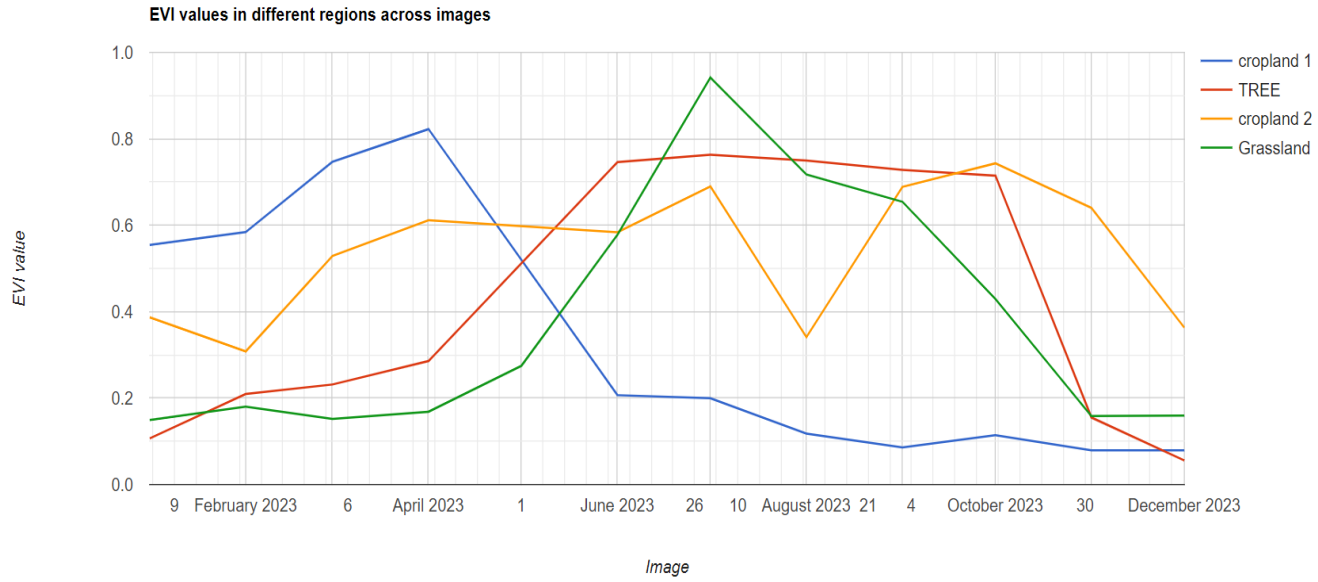

Figure 12 EVI region timeseries

RESULTS

Spectral indices interpretation

NDVI

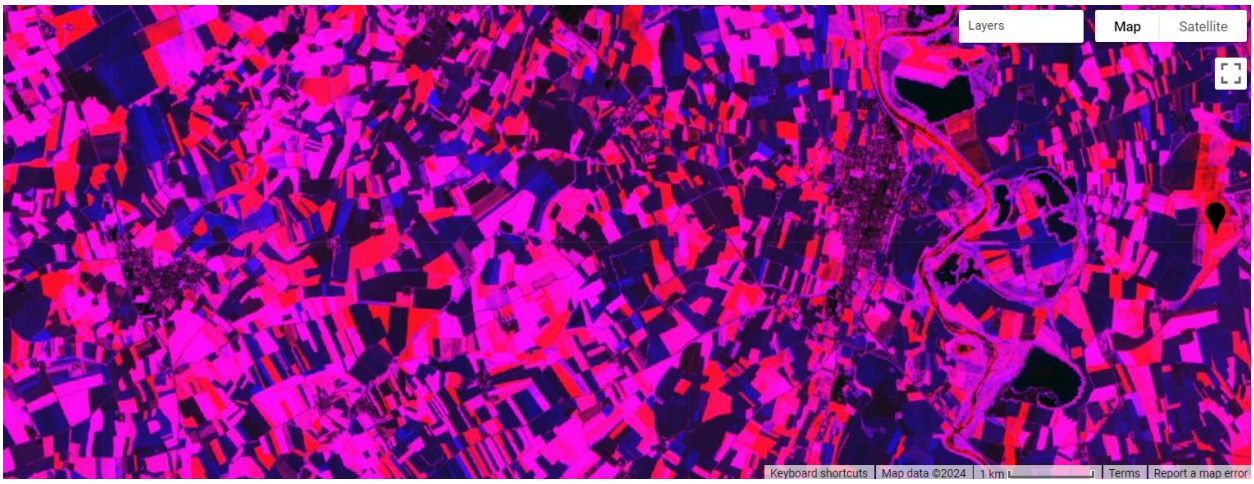

Figure 13 NDVI

The NDVI time series bands represent different months, with April designated as red, June as green, and October as blue. From the above image, it is evident that most croplands are grown and ready for harvest in April. Additionally, there are late-season croplands that exhibit high NDVI values in October. Interestingly, there are no cultivated croplands visible in June.

Figure 14 depicts the tree region. Generally, lighter colors indicate higher NDVI values throughout the year. The inclination towards blue demonstrates that the highest NDVI values occur in October, as evident in the NDVI time series plot.

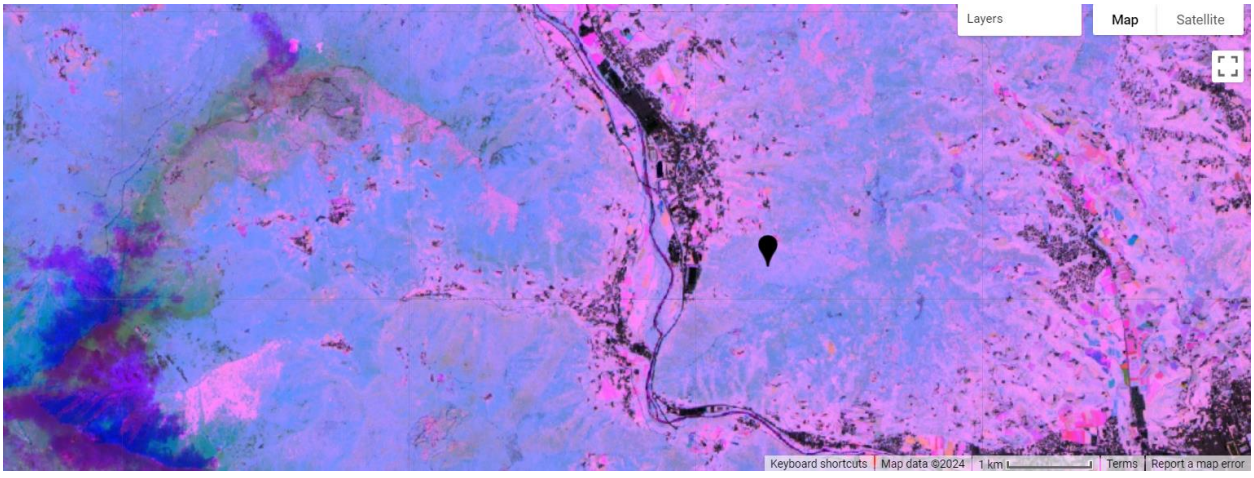

Figure 14 NDVI, forest region

Similarly, the grassland shows its growth and peak NDVI values in April, as indicated by the red color assigned to that month.

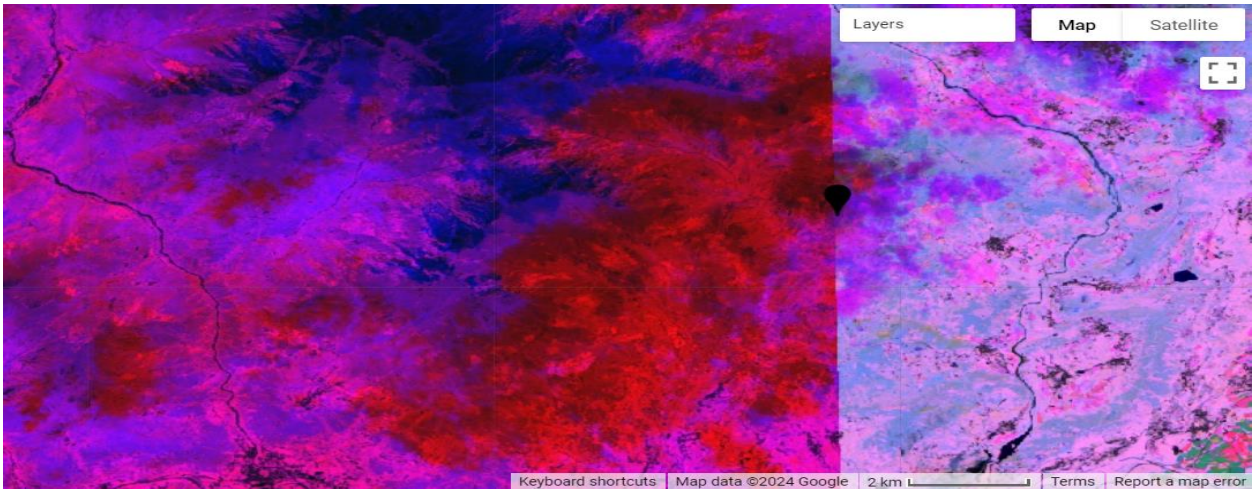

Figure 15 NDVI, Grasslands region

EVI

Conducting the same analysis with the EVI results further supports our validation.

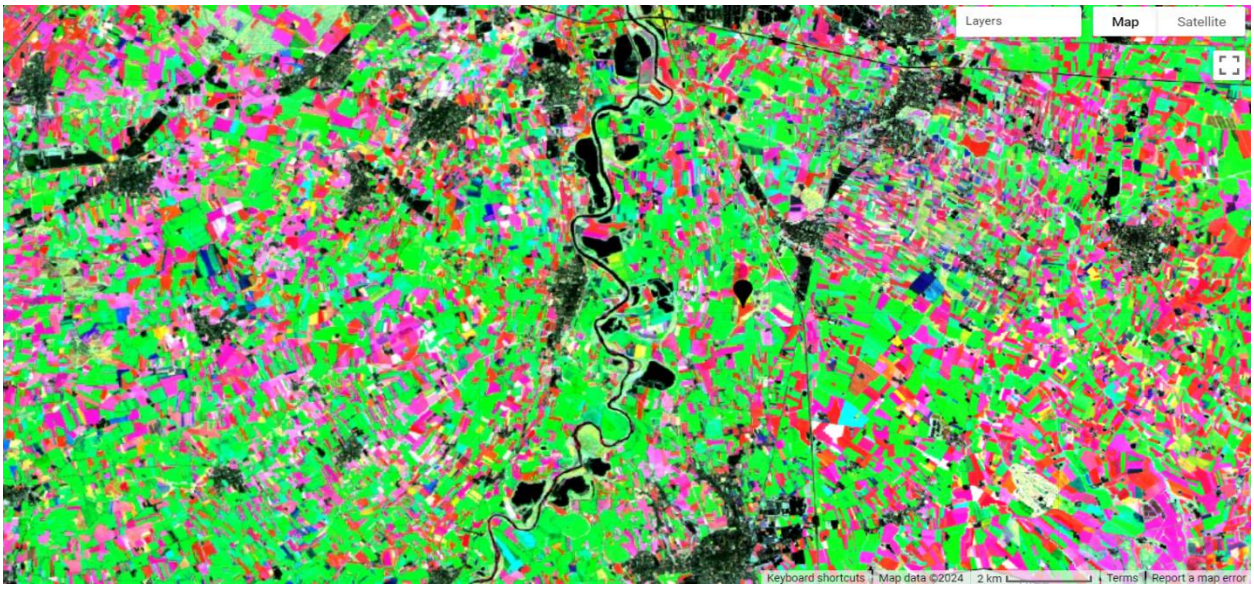

Figure 16 EVI

By assigning RED to April, GREEN to June, and BLUE to October, Figure 16 reveals some differences compared to NDVI. Specifically, the EVI index indicates that most agricultural fields are predominantly grown during the summer and late spring. In contrast, the NDVI reflects significant growth during spring and autumn.

Let's examine the forest and grassland regions.

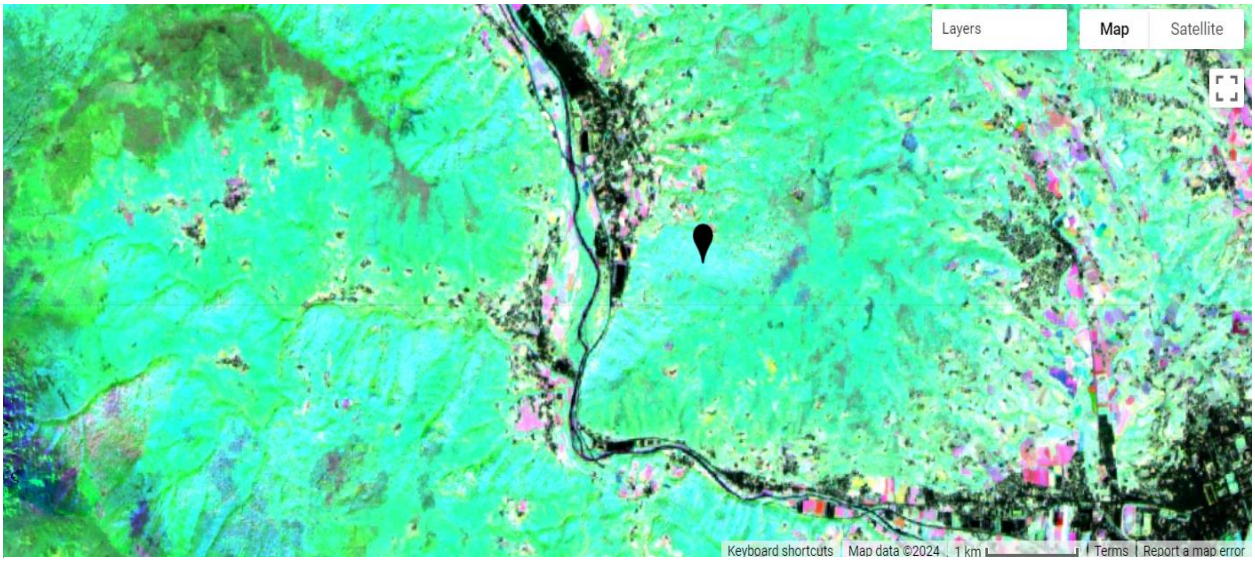

Figure 17 EVI, forest region

The EVI for trees exhibits a pattern similar to that of NDVI. The lighter colors indicate consistently high values throughout the year, with a blend of blue and green reflecting peak values in late summer and early autumn.

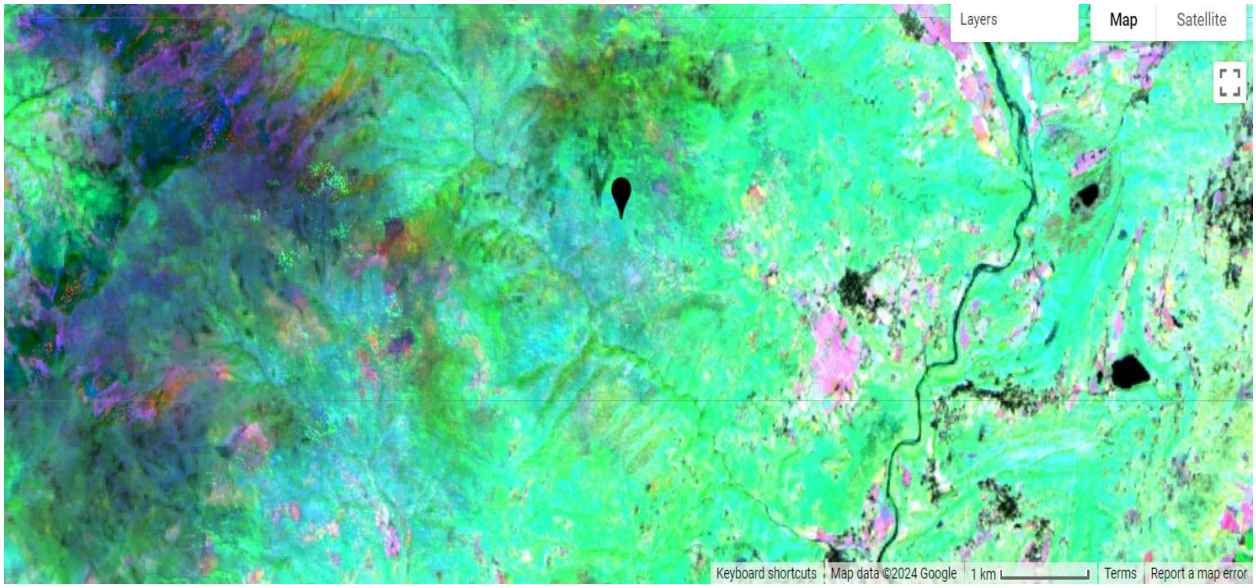

Figure 18 EVI grassland

As shown in Figure 10, the lowest EVI value for grassland occurs in April, while values increase during the summer and decrease slightly afterward. Therefore, the absence of the RED color in Figure 18 is justifiable, as the mix of GREEN and BLUE reflects the grassland's elevated EVI values during the summer and autumn months.

Seasonality analysis

April analysis

By filtering the merged NDVI image specifically for April, only the images acquired during that month were selected. A median composite was applied to minimize the influence of outliers. The resulting NDVI median image for April was then updated with temporal properties, including the start time and a formatted index for easier identification. Finally, the image was clipped and mapped for further analysis. Figure 19 shows the NDVI values which vary from -1 to 1.

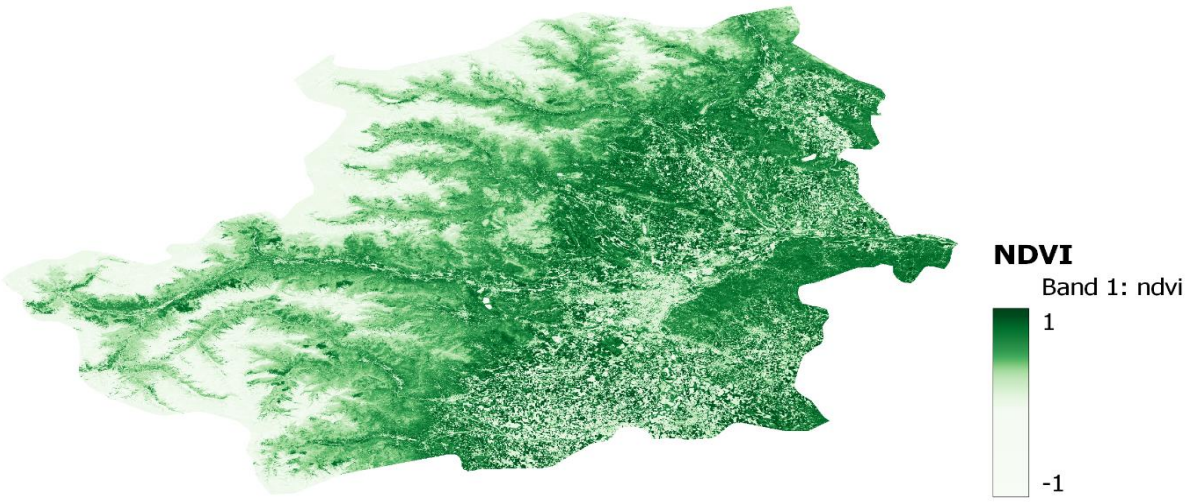

Figure 19 NDVI APRIL 2023

Similarly, an EVI map was generated by applying the same filtering and processing techniques. Images acquired in April were selected, and a median composite was utilized to reduce the impact of outliers. The resulting EVI median image for April was updated with temporal properties, including the start time and a formatted index for easy identification. This image was also clipped and mapped for further analysis.

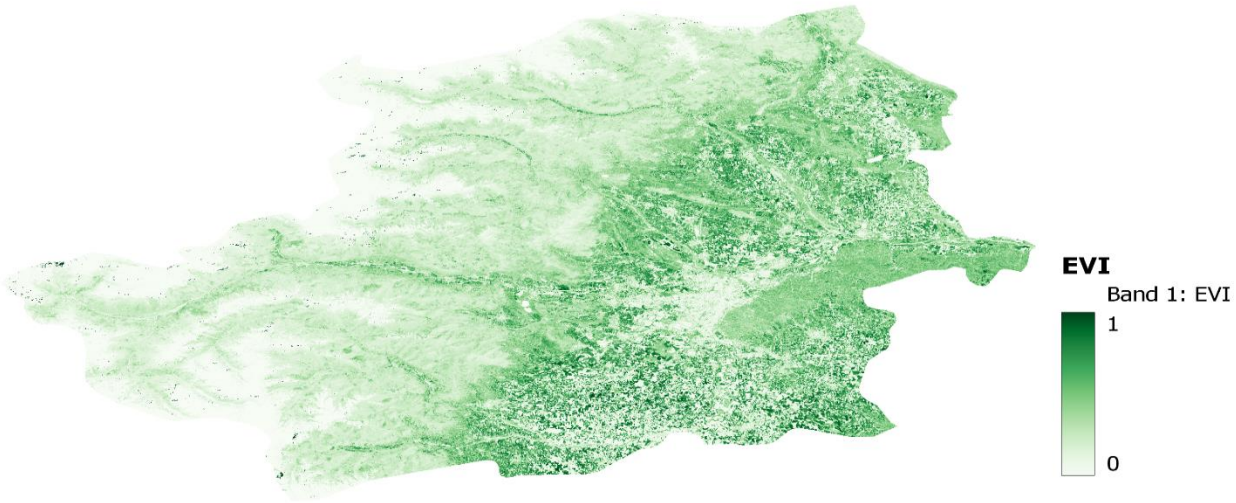

Figure 20 EVI APRIL 2023

.

Since the EVI values are generally lower than those of NDVI and effectively minimize the effects of soil, the resulting map visualizations differ between the two indices. To classify the region into three categories—Trees, Grassland, and Cropland—using both EVI and NDVI values, we can apply specific thresholds to the spectral indices.

In April, as shown in Figure 11, Cropland 1 and Cropland 2 exhibit high NDVI values exceeding 0.8. Therefore, setting a minimum threshold of 0.7 is appropriate for Cropland classification. NDVI values for Trees range from 0.45 to 0.7, while those for Grassland fall between 0.2 and 0.45. It's important to note that NDVI values below 0.2 indicate dead or unhealthy vegetation, which does not contribute to carbon storage.

Figure 21 illustrates the results of this classification.

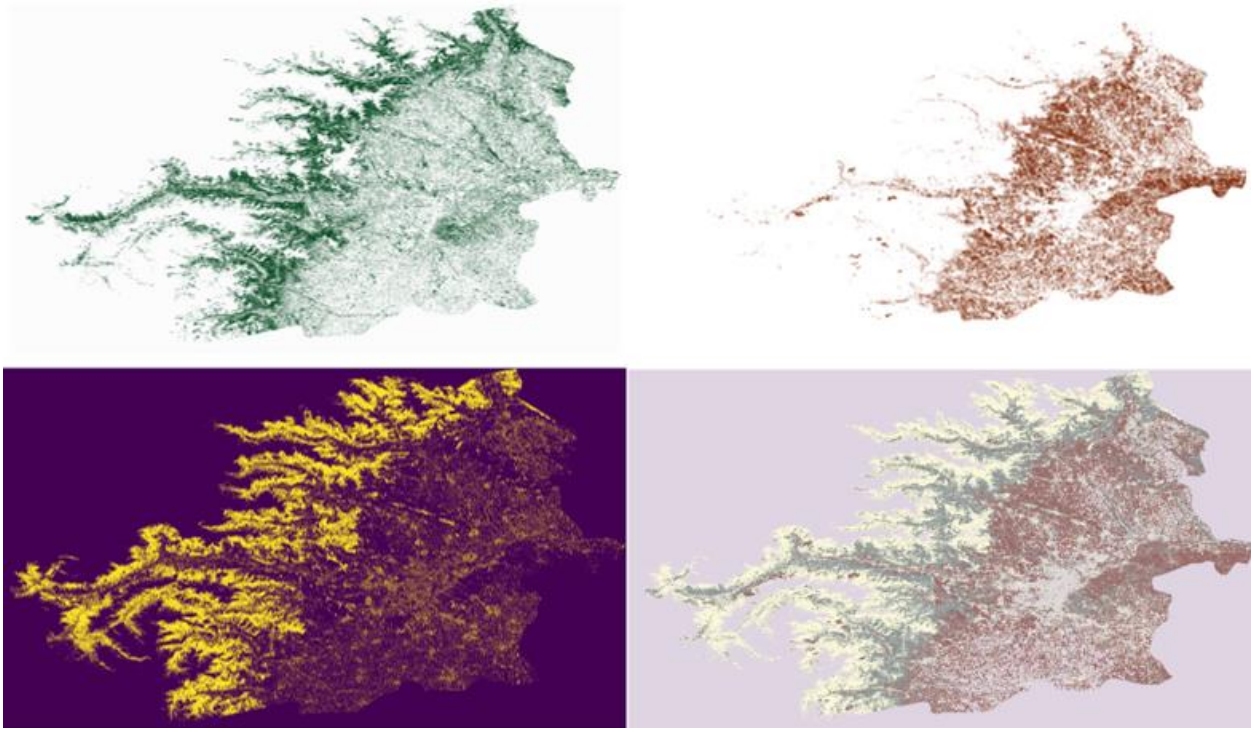

Figure 21 classification derived by NDVI in April. upper left: Trees, upper right: Cropland, lower left: Grassland, lower right: all three classes in region

Setting thresholds for EVI differs from those for NDVI. In April, as shown in Figure 12, Cropland 1 and Cropland 2 exhibit high EVI values exceeding 0.65. Therefore, establishing a minimum threshold of 0.65 is appropriate for classifying Cropland. The EVI values for Trees range from 0.25 to 0.5, while Grassland values fall between 0.1 and 0.25. Figure 22 illustrates the results of this classification.

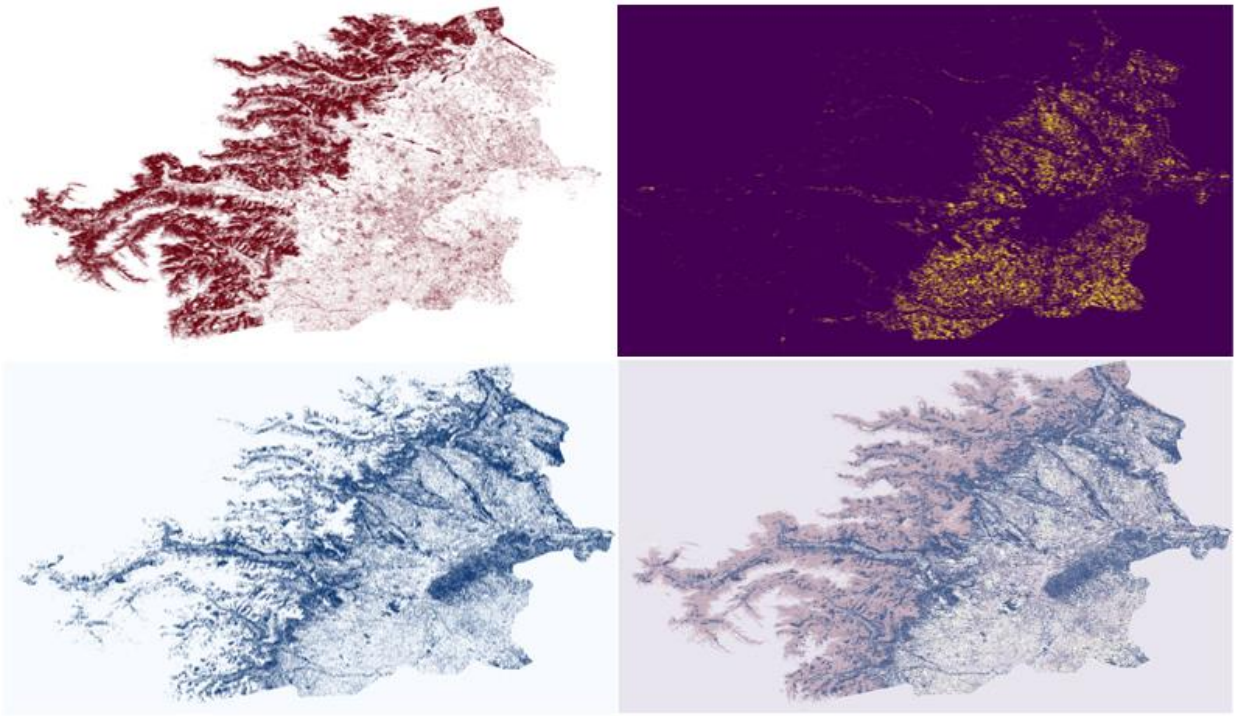

Figure 22 derived by EVI in April. upper left: Trees, upper right: Cropland, lower left: Grassland, lower right: all three classes in region

October analysis

By filtering the merged NDVI image for October, only the images acquired during this month were selected. A median composite was created to minimize the impact of outliers. The NDVI median image for October was then updated with time properties, which include the start time and a formatted index for easy identification. Finally, the image was clipped and mapped accordingly.

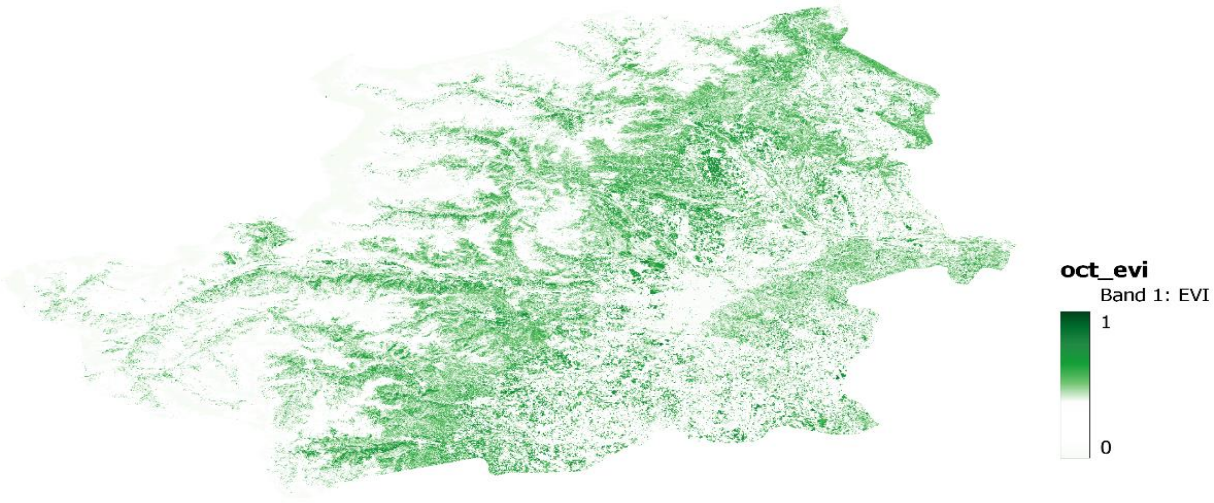

Figure 23 EVI OCTOBER 2023

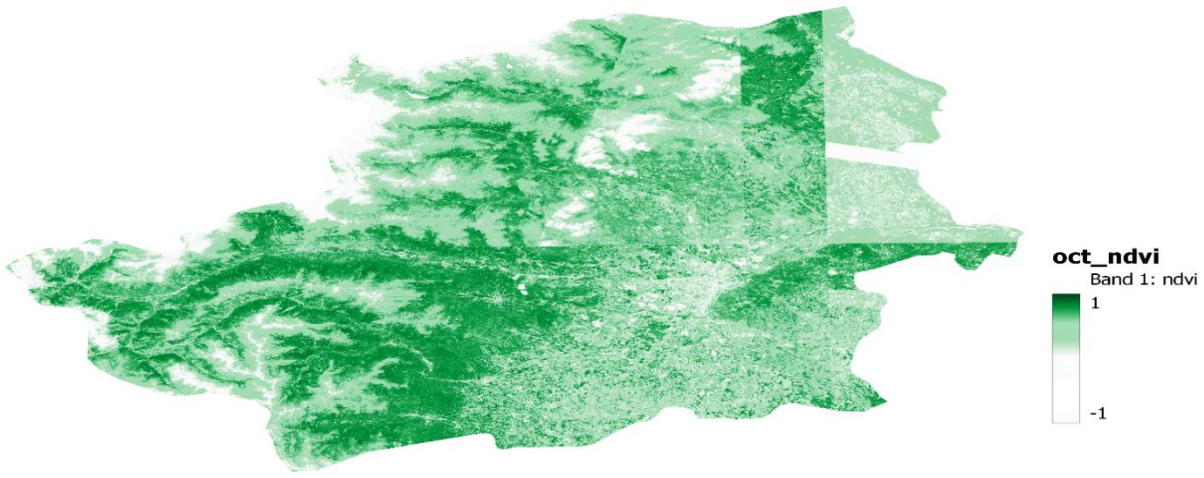

Figure 24 NDVI OCTOBER 2023

The classification of vegetation types in October was carried out by establishing new thresholds based on the April values. For NDVI in October, trees exhibit the highest values, so the threshold for trees was set above 0.8. Considering Figures 11 and 12, two distinct types of crops were identified: the threshold for Crop Type 1 ranges from 0.7 to 0.75, while Crop Type 2 falls between 0.15 and 0.25. Lastly, the threshold for grassland was established between 0.4 and 0.6.

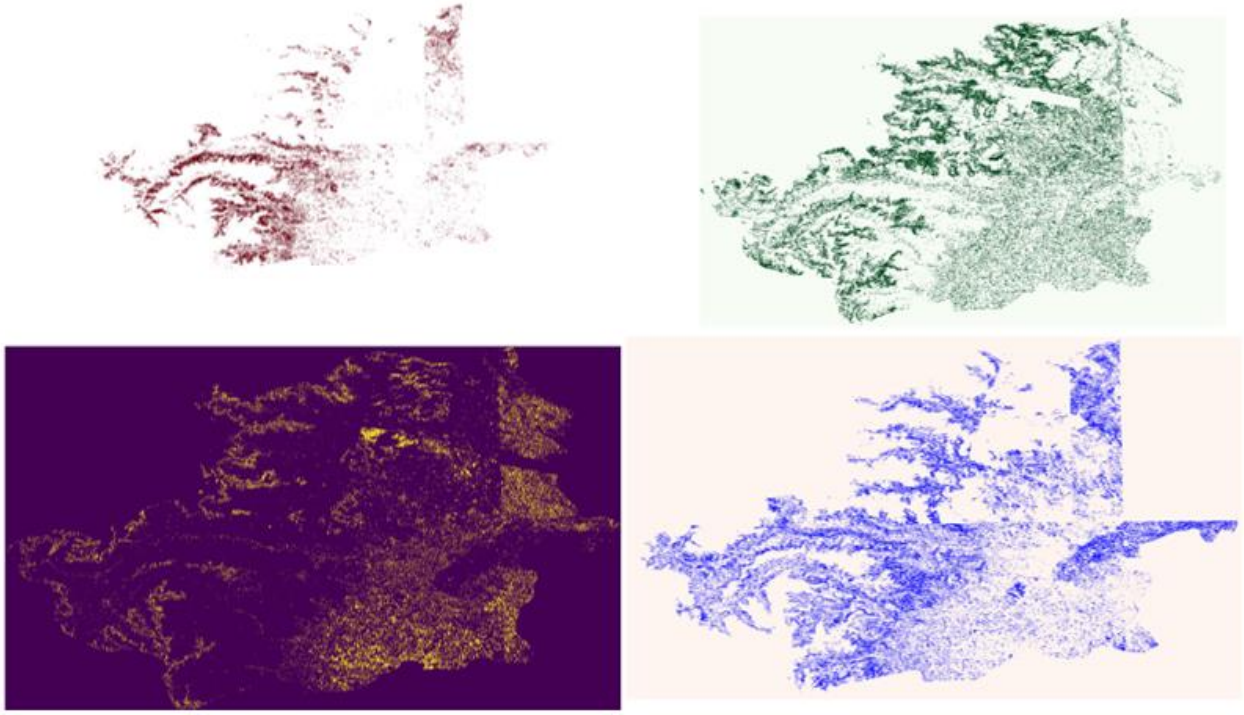

Figure 25 classification derived by NDVI in October. upper left: Trees, upper right: Grassland, lower left: Cropland 1, lower right: Cropland 2

For the classification based on EVI in October, the threshold for Crop Type 1, which has the highest EVI values, was set above 0.7. The threshold for trees was established between 0.5 and 0.7, while grassland was classified with values ranging from 0.3 to 0.49. Finally, Crop Type 2 was assigned a threshold between 0.08 and 0.15. The results of this classification are illustrated in Figure 25.

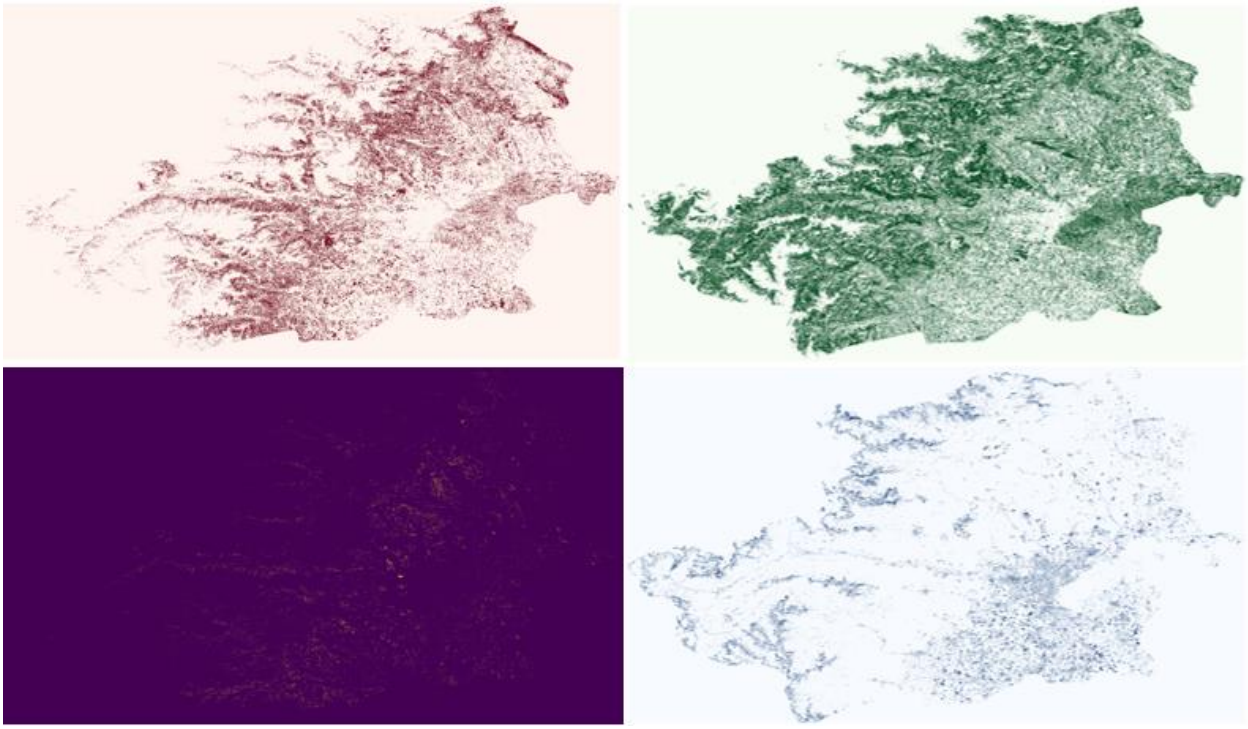

Figure 26 classification derived by EVI in October. upper left: Trees, upper right: Grassland, lower left: Cropland 1, lower right: Cropland 2

classification

By considering the intersection of both NDVI and EVI for each class, the uncertainty is reduced, resulting in the generation of a highly reliable map for both April and October. Figures 27-29 display the area of each class in April, while Figures 30-32 present the area of each class in October.

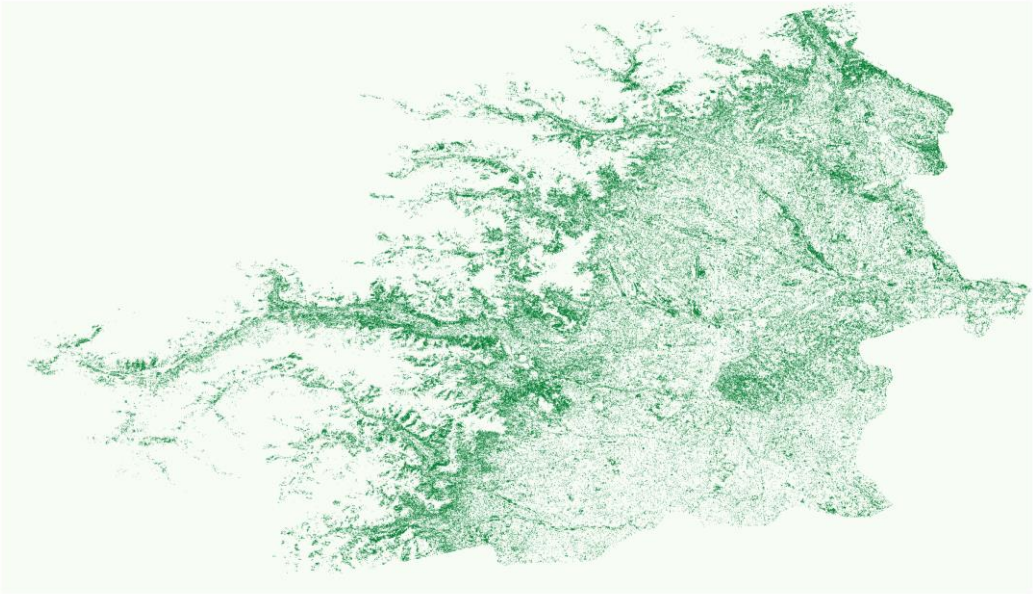

Figure 27 area of trees for April 2023

Figure 28 area of croplands for April 2023

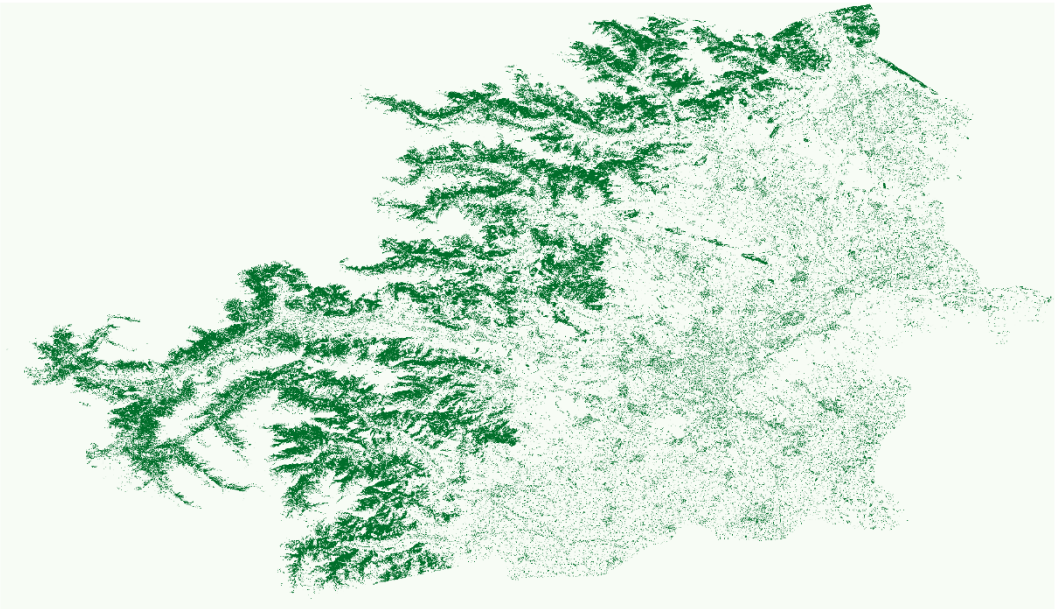

Figure 29 area of grasslands for April 2023

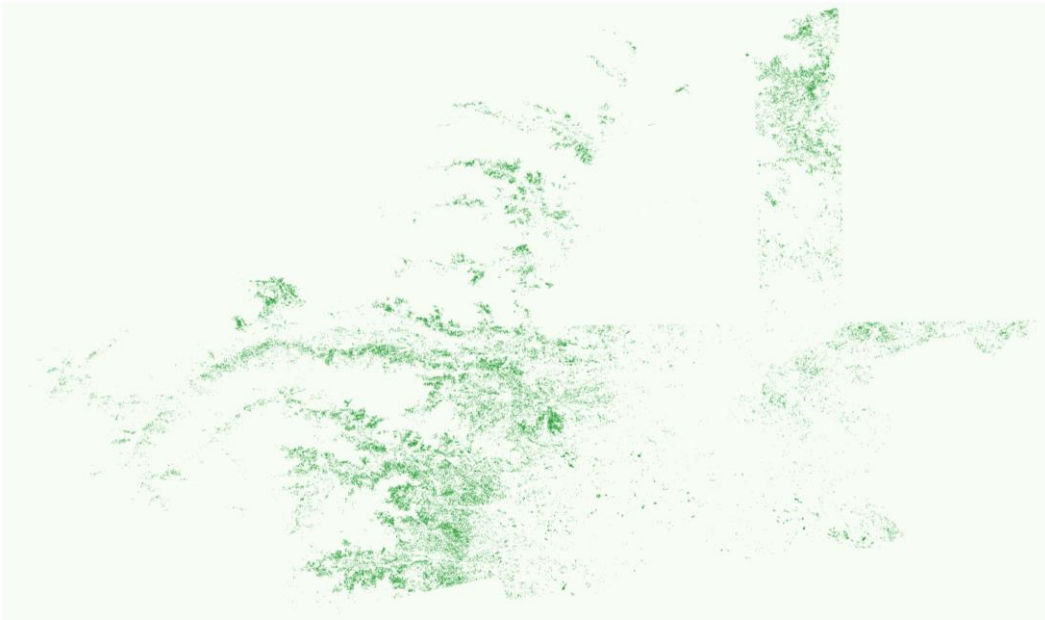

Figure 30 area of trees for October 2023

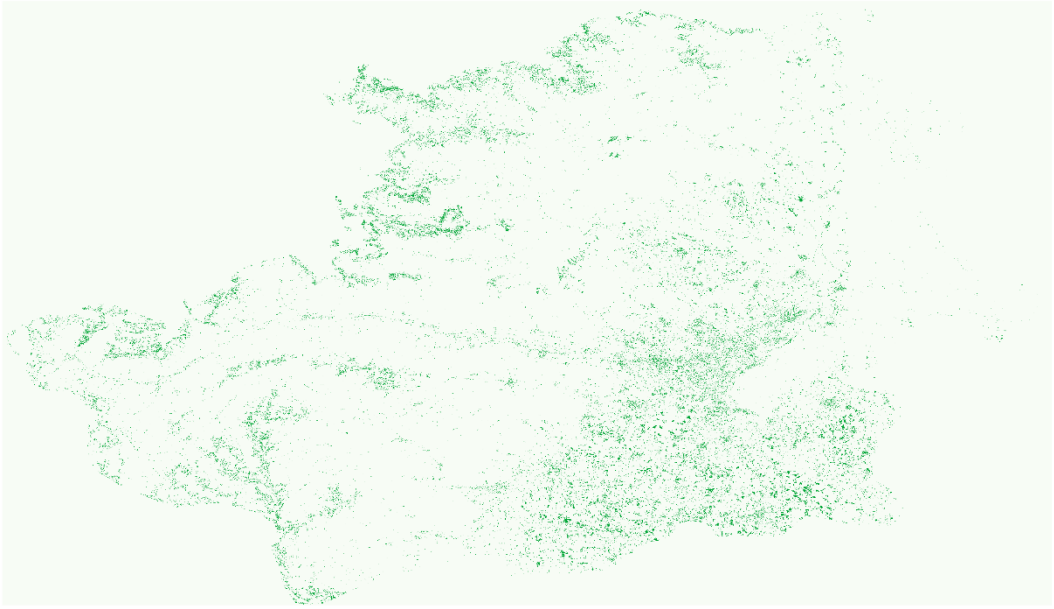

Figure 31 area of croplands for October 2023

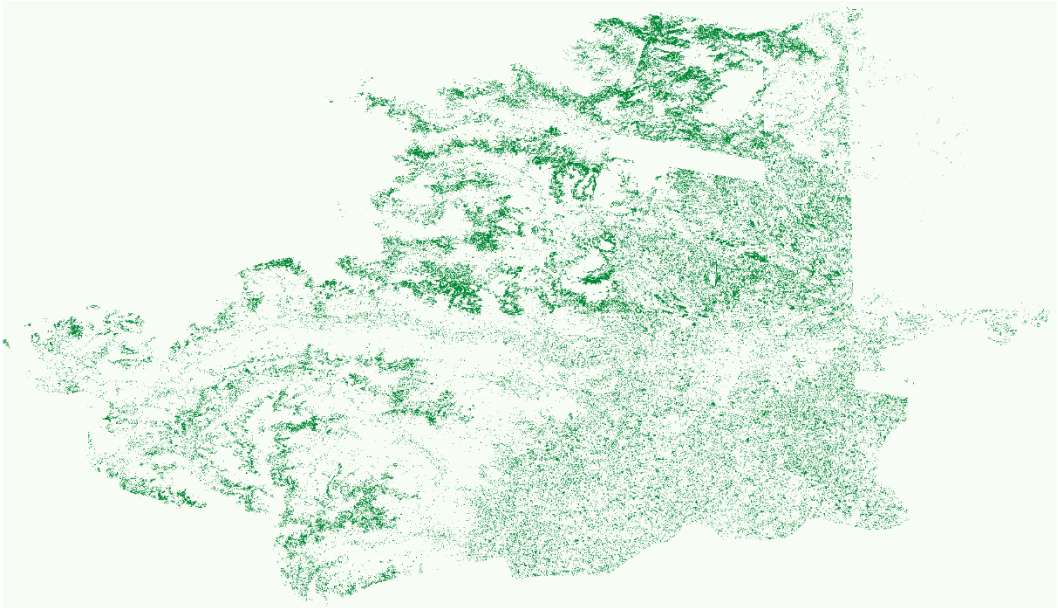

Figure 32 area of grasslands for October 2023

Area calculation

Using the pixelArea function in Google Earth Engine, the area of each class was obtained. The following table represents these values.

Table 1 land cover area of April and October 2023

Land Cover Type	April (ha)	October (ha)
Trees	120,185.7316	30,033.37185
Grassland	155,834.3086	90,917.3979
Cropland	50,329.47522	24,562.6298

Discussion

Carbon storage estimation

The analysis of vegetation types (trees, grasslands, croplands) in Turin's metropolitan area for carbon storage estimation, utilizing remote sensing data, has revealed significant seasonal variability between April and October. This variability is largely influenced by land cover dynamics, including agricultural cycles, seasonal vegetation growth, and land management practices.

The carbon storage potential for April and October was assessed using general carbon density values for temperate forests, grasslands, and croplands, in accordance with IPCC guidelines and established scientific literature.(Krug et al., n.d.)(Scarascia-Mugnozza et al., 2000)(Conant et al., 2001) (Post & Kwon, 2008).

The carbon density values used for this estimation are as follows:

- **Trees**: 120 tons of carbon per hectare (tC/ha)
- **Grasslands**: 50 tC/ha
- **Croplands**: 75 tC/ha

These values align with IPCC guidelines and relevant scientific literature, providing a solid foundation for estimating carbon storage potential in the Turin metropolitan area.

Carbon Storage Estimation for April

In April, the total area of trees, grasslands, and croplands amounted to approximately 326,349.5155 hectares. Using the carbon density values, the total carbon storage for April was estimated as:

Table 2 Carbon storage in April 2023

Land Cover Type	Area (ha)	Carbon Density (tC/ha)	Total Carbon Storage (tC)
Trees	120,185.7316	120	14,422,287.79
Grasslands	155,834.3086	50	7,791,715.43
Croplands	50,329.47522	75	3,774,710.64

This results in a total carbon storage of 25,988,713.86 tons of carbon (tC) for April.

Carbon Storage Estimation for October

For October, the total area of the same vegetation types decreased to 145,513.3995 hectares. The estimated total carbon storage for October is:

Table 3 Carbon storage in October 2023

Land Cover Type	Area (ha)	Carbon Density (tC/ha)	Total Carbon Storage (tC)
Trees	30,033.37185	120	3,604,004.62
Grasslands	90,917.3979	50	4,545,869.90
Croplands	24,562.6298	75	1,842,197.24

The total carbon storage for October is 9,992,071.76 tons of carbon (tC).

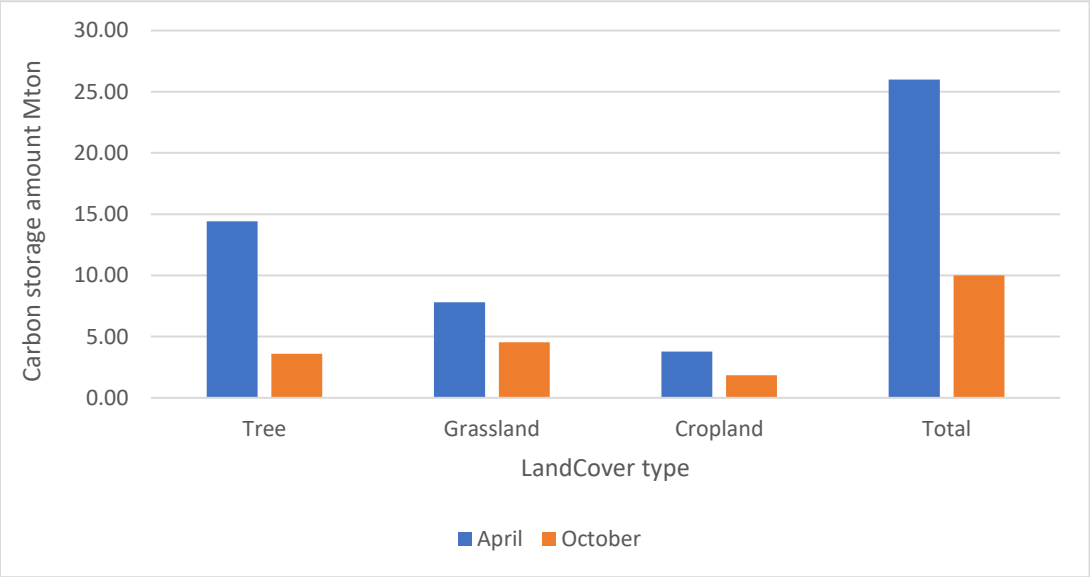

Figure 33 Carbon storage amount of different landcover types in April and October 2023

Carbon storage fluctuations

The study evaluated carbon storage changes under various land cover types, with emphasis on April and October as representative months for spring and autumn, respectively. The data in Figures 9 and 10 show a decrease in NDVI and EVI values from April to October, which indicates a decline in carbon uptake across different land covers during the latter part of the year.

Tree Cover:

- In April, trees exhibited high carbon storage with NDVI values between 0.45 and 0.7 and EVI between 0.25 and 0.5. However, by October, these values slightly decreased, indicating reduced photosynthetic activity and, consequently, a decrease in carbon storage.
- The reduction in spectral indices from spring to autumn suggests that trees' carbon sequestration rates, although still significant, are lower in autumn as compared to spring. This decrease could be attributed to factors like leaf senescence and reduced sunlight. The overall decline is around 5-10%, suggesting that even though trees are perennial, seasonal changes impact their carbon uptake which decreased more than 75%.

Grasslands:

- Grasslands showed variability, with NDVI and EVI values ranging from 0.2 to 0.45 and 0.1 to 0.25 in April, reflecting moderate carbon uptake. However, as indicated in Figures 9 and 10, by October, these values declined further to 0.15 to 0.25, marking a sharp reduction in carbon storage.
- The approximately 25-30% reduction in NDVI reflects the dormancy of grasslands during autumn, a typical characteristic as the growing season ends. This seasonal drop significantly impacts the carbon sequestration potential of grasslands by 50% (from 7.8 Mton to 4.5 Mton).

Croplands:

- Croplands experienced the most dynamic shifts in NDVI and EVI values. In April, values above 0.8 and 0.65 indicated peak carbon storage during the growing phase. However, by October, NDVI and EVI values plummeted to as low as 0.15 to 0.25, primarily due to post-harvest conditions.
- Late-season crops maintained slightly higher NDVI and EVI values (0.7 to 0.75) in October, suggesting continued carbon sequestration. However, for the second type of crop, NDVI and EVI values dropped significantly, falling below 0.2, which highlights a substantial reduction in overall carbon storage.
- This significant decrease, particularly in the second crop type, emphasizes the seasonal nature of croplands. Agricultural practices like harvesting lead to a 50% reduction in carbon storage by autumn, demonstrating the need for improved land management techniques such as cover cropping and crop rotation to optimize carbon retention.

The findings highlight how crop harvesting drastically impacts carbon storage, emphasizing the need for agricultural management strategies that mitigate these fluctuations. Introducing cover crops or diversifying planting seasons could extend the periods of carbon uptake in croplands.

Comparison Across Land Cover Types

Tree cover, while often regarded as a stable contributor to carbon sequestration, showed a slight decrease in carbon storage from spring to autumn, as indicated by the lower NDVI values in October compared to April. This suggests that trees, despite their perennial nature, experience reduced photosynthetic activity and carbon uptake in autumn.

Grasslands, on the other hand, demonstrated relatively consistent carbon storage between April and October, with only minor reductions in NDVI and EVI values. This suggests that grasslands, while dependent on seasonal growth cycles, maintain more consistent carbon storage throughout the growing season, likely due to their resilience to environmental fluctuations.

Croplands exhibited the most significant fluctuations in carbon storage due to agricultural practices. As seen in the spectral indices, croplands had high NDVI and EVI values in April, indicating peak carbon uptake. However, by October, cropland values dropped dramatically, especially for the second crop type,

where NDVI and EVI values fell below 0.2. This sharp reduction highlights the impact of harvesting and seasonal crop cycles on carbon storage.

Thus, while croplands are highly productive in terms of carbon sequestration during their growing phase, their overall contribution to long-term carbon storage is diminished by harvesting activities. Sustainable practices, such as crop rotation or cover cropping, could mitigate these seasonal reductions and optimize cropland carbon retention.

Spectral Indices and Vegetation Monitoring

The combined use of NDVI and EVI in this research effectively captured vegetation dynamics, as these indices are well-established in remote sensing for their sensitivity to vegetation conditions. NDVI is widely recognized for assessing vegetation health based on chlorophyll content, while EVI enhances the signal-to-noise ratio, particularly in densely vegetated areas, by minimizing atmospheric interferences.

The analysis of monthly time series data for both indices revealed seasonal patterns of vegetation, with April and October representing the peak vegetative phases of spring and autumn respectively. The NDVI values during these months showed higher readings, particularly in agricultural areas, indicating active plant growth and photosynthetic activity. The correlation of NDVI and EVI data with seasonal variations provides a reliable basis for monitoring carbon uptake by vegetation, which plays a critical role in carbon sequestration.

In addition, the comparison between April and October demonstrated that croplands exhibited significant NDVI drops during harvest seasons, while forests and grasslands maintained relatively stable values. The use of thresholding enabled the classification of different land cover types, confirming the presence of different crop cycles and natural vegetation with varying carbon storage potential.

Classification of Land Cover Types

The classification of land cover using NDVI and EVI allowed for an accurate estimation of the area occupied by trees, grasslands, and croplands. These vegetation types are vital components of carbon sequestration systems, with forests being the most significant due to their longer life cycles and substantial biomass.

For instance, the study identified significant differences in NDVI and EVI values for trees and grasslands. The data showed that trees consistently retained high values throughout the year, reflecting their sustained photosynthetic activity and carbon storage potential. On the other hand, grasslands demonstrated higher values in the spring, with a steady decline through the summer and fall, likely due to environmental conditions such as temperature and precipitation.

Moreover, the results showed a clear distinction between NDVI and EVI between cropland types, where late-season crops retained higher values in October due to prolonged growth cycles. Such distinctions are

essential for understanding the role of agricultural systems in carbon sequestration, especially when considering different cropping patterns and management practices.

Challenges in Biomass Estimation and Remote Sensing

Despite the advancements in remote sensing and the promising results achieved in this study, there remain several challenges in the accurate estimation of biomass and carbon stocks. These include the complexity of vegetation structure, cloud cover interference, and the non-linear relationship between spectral indices and biomass.

Vegetation structure and composition can introduce variability in the indices' readings, particularly in heterogeneous landscapes where forests, agriculture, and grasslands coexist. The differences in plant types, canopy structures, and even age can affect the reflectance captured by satellites, leading to discrepancies in the NDVI and EVI data.

Additionally, cloud cover, especially during certain seasons, can limit the availability of cloud-free imagery, which affects the temporal consistency of the data. Although the median composite technique was employed to minimize these interferences, this limitation still presents challenges in biomass monitoring.

Area Calculation and Carbon Sequestration Potential

The area calculation based on binary classification images provided estimates of tree, grassland, and cropland coverage in hectares. The results indicated that in April, approximately 120,186 hectares were covered by trees, while grasslands and croplands occupied 155,834 and 50,329 hectares, respectively.

In October, the tree and cropland areas decreased due to seasonal shifts, with grasslands remaining dominant in terms of spatial coverage.

These area estimates are significant for assessing the carbon sequestration potential of the region. Trees, with their dense biomass and longer life cycles, serve as more reliable carbon sinks compared to agricultural areas, which undergo seasonal changes. Grasslands, while covering a larger area, have lower biomass per hectare, thus contributing less to long-term carbon storage compared to forested areas.

Furthermore, the decline in cropland area in October highlights the importance of understanding agricultural cycles in carbon assessments. Harvesting and land management practices such as plowing can reduce carbon sequestration temporarily, while crop growth contributes to carbon absorption during the growing season.

Validation and Future Directions

The study utilized Copernicus CORINE Land Cover data for validation of the classification results, confirming the accuracy of the land cover types. This combination of satellite-derived indices and external land cover data sources ensured the robustness of the classification approach, which is critical for carbon stock estimation.

In the future, additional validation through ground-based measurements would enhance the accuracy of biomass and carbon estimates, as remote sensing alone cannot capture the full complexity of vegetation structure and carbon content. The integration of LiDAR data or high-resolution imagery could provide greater detail on vegetation height and structure, improving carbon estimation models.

Furthermore, incorporating soil carbon measurements would provide a more holistic view of the region's carbon stock, as soil represents a significant component of the global carbon cycle. Expanding the temporal scope to include multi-year data would also allow for better understanding of interannual variability in vegetation and carbon sequestration potential.

Uncertainty in Estimations

Several uncertainties exist in the process of estimating carbon storage using remote sensing methods.

- Vegetation Indices: While NDVI and EVI are commonly used, their sensitivity to seasonal changes may introduce inaccuracies when assessing heterogeneous landscapes. These indices primarily focus on chlorophyll content and may not fully account for different vegetation structures, soil conditions, or mixed land use areas. Additionally, their effectiveness in dense forests or sparse grasslands can vary, sometimes leading to over- or underestimation of carbon storage.
- Seasonal and Climatic Variations: Fluctuations in weather, such as precipitation and temperature, affect vegetation growth and the accuracy of remote sensing data. Cloud cover, which obstructs satellite views, further complicates the reliability of NDVI and EVI readings, necessitating data corrections and interpolations.
- Spatial Resolution: The differing spatial resolutions between satellite imagery (such as Sentinel-2 and Landsat) can affect the precision of carbon stock estimations. While high-resolution images provide detailed data, they may not be available consistently across all time frames, leading to potential data gaps or inconsistencies in analysis.
- Ground-Truthing: Although satellite imagery offers extensive coverage, calibration with on-the-ground measurements (ground-truthing) is crucial to enhance accuracy. The lack of sufficient ground-truthing data can introduce discrepancies in remote sensing-based carbon stock calculations.

Conclusion

This research has demonstrated the significant role of remote sensing in monitoring carbon storage across various land cover types, utilizing a comprehensive dataset consisting of 198 images from Sentinel-2, 30 from Landsat 8, and 34 from Landsat 9. By analyzing spectral indices such as the Normalized Difference Vegetation Index (NDVI) and the Enhanced Vegetation Index (EVI), this study has provided valuable insights into the dynamics of carbon sequestration throughout different seasons.

Tree cover has been identified as a critical contributor to carbon storage in the region. However, the analysis revealed a significant reduction of over 75% in carbon storage from April to October, as indicated in Tables 2 and 3. This substantial decline underscores the impact of seasonal changes on tree carbon sequestration and emphasizes the need for effective forest management strategies to enhance their contribution to carbon credits. Sustainable practices that promote healthy forest ecosystems can bolster tree cover's role in climate change mitigation.

Grasslands and croplands also exhibited considerable reductions in carbon storage, each experiencing declines of approximately 50% over the same period. This decrease highlights the challenges faced by these land covers in maintaining their carbon credit potential, particularly as seasonal growth patterns shift. Effective management practices, including rotational grazing and cover cropping in grasslands, and adopting sustainable agricultural practices in croplands, can improve their carbon sequestration capabilities and enhance their contributions to carbon credit markets.

In summary, the findings of this study contribute valuable knowledge to the carbon credit domain, demonstrating how different land cover types influence carbon storage dynamics. While tree cover has historically been viewed as a reliable carbon sink, its recent drastic reductions necessitate focused management interventions. Both grasslands and croplands, with their notable carbon storage reductions, present opportunities for improvement through sustainable practices. By optimizing land management and leveraging remote sensing technologies, it is possible to enhance carbon credits in the region, thereby supporting broader climate goals and contributing to sustainable development.

References

Ahmed, Z., Nalley, L., Brye, K., Steven Green, V., Popp, M., Shew, A. M., & Connor, L. (2023). Winter-time cover crop identification: A remote sensing-based methodological framework for new and rapid data generation. *International Journal of Applied Earth Observation and Geoinformation*, *125*, 103564. https://doi.org/https://doi.org/10.1016/j.jag.2023.103564

Baret, F., Guyot, G., & Major, D. J. (1989). Crop biomass evaluation using radiometric measurements. *Photogrammetria*, *43*(5), 241–256. https://doi.org/https://doi.org/10.1016/0031-8663(89)90001-X

Barrett, F., McRoberts, R. E., Tomppo, E., Cienciala, E., & Waser, L. T. (2016). A questionnaire-based review of the operational use of remotely sensed data by national forest inventories. *Remote Sensing of Environment*, *174*, 279–289. https://doi.org/https://doi.org/10.1016/j.rse.2015.08.029

Begue, A., Vintrou, E., Saad, A., & Hiernaux, P. (2014). Differences between cropland and rangeland MODIS phenology (start-of-season) in Mali. *International Journal of Applied Earth Observation and Geoinformation*, *31*, 167–170. https://doi.org/https://doi.org/10.1016/j.jag.2014.03.024

Brown, S., Gillespie, A., & Lugo, A. (1989). Biomass Estimation Methods for Tropical Forests with Applications to Forest Inventory Data. *Forest Science*, *35*, 881–902. https://doi.org/10.1093/forestscience/35.4.881

carbon credit. (n.d.). Https://Www.Merriam-Webster.Com/Dictionary/Carbon%20credit.

Conant, R., Paustian, K., & Elliott, E. (2001). Grassland Management and Conversion into Grassland: Effects on Soil Carbon. *Ecoa*, *11*, 343. https://doi.org/10.1890/1051-0761(2001)011[0343:GMACIG]2.0.CO;2

Daughtry, C. S. T., Gallo, K. P., Goward, S. N., Prince, S. D., & Kustas, W. P. (1992). Spectral estimates of absorbed radiation and phytomass production in corn and soybean canopies. *Remote Sensing of Environment*, *39*(2), 141–152. https://doi.org/https://doi.org/10.1016/0034-4257(92)90132-4

Dhanaraju, M., Chenniappan, P., Ramalingam, K., Pazhanivelan, S., & Kaliaperumal, R. (2022). Smart Farming: Internet of Things (IoT)-Based Sustainable Agriculture. *Agriculture*, *12*(10). https://doi.org/10.3390/agriculture12101745

Duncanson, L., Kellner, J. R., Armston, J., Dubayah, R., Minor, D. M., Hancock, S., Healey, S. P., Patterson, P. L., Saarela, S., Marselis, S., Silva, C. E., Bruening, J., Goetz, S. J., Tang, H., Hofton, M., Blair, B., Luthcke, S., Fatoyinbo, L., Abernethy, K., … Zgraggen, C. (2022). Aboveground biomass density models for NASA's Global Ecosystem Dynamics Investigation (GEDI) lidar mission. *Remote Sensing of Environment*, *270*, 112845. https://doi.org/https://doi.org/10.1016/j.rse.2021.112845

Fassnacht, F. E., Schmidt-Riese, E., Kattenborn, T., & Hernández, J. (2021). Explaining Sentinel 2-based dNBR and RdNBR variability with reference data from the bird's eye (UAS) perspective. *International Journal of Applied Earth Observation and Geoinformation*, *95*, 102262. https://doi.org/https://doi.org/10.1016/j.jag.2020.102262

Foody, G. M., Palubinskas, G., Lucas, R. M., Curran, P. J., & Honzak, M. (1996). Identifying terrestrial carbon sinks: Classification of successional stages in regenerating tropical forest from Landsat TM data. *Remote Sensing of Environment*, *55*(3), 205–216. https://doi.org/https://doi.org/10.1016/S0034-4257(95)00196-4

Guidance on the mechanism established by Article 6, paragraph 4, of the Paris Agreement. (n.d.).

Gupta, R. K., Prasad, T. S., & Vijayan, D. (2000). Relationship between LAI and NDVI for IRS LISS and Landsat TM bands. *Advances in Space Research*, *26*(7), 1047–1050. https://doi.org/https://doi.org/10.1016/S0273-1177(99)01115-1

Janga, B., Asamani, G., Sun, Z., & Cristea, N. (2023). A Review of Practical AI for Remote Sensing in Earth Sciences. *Remote Sensing*, *15*, 4112. https://doi.org/10.3390/rs15164112

Jin, S., & Sader, S. A. (2005). MODIS time-series imagery for forest disturbance detection and quantification of patch size effects. *Remote Sensing of Environment*, *99*(4), 462–470. https://doi.org/https://doi.org/10.1016/j.rse.2005.09.017

Kazak, J., Malczyk, J., Castro, D. G., & Szewrański, S. (2016). Carbon sequestration in forest valuation. *Real Estate Management and Valuation*, *24*(1), 76–86. https://doi.org/10.1515/remav-2016-0007

Khavarian Nehzak, H., Aghaei, M., Mostafazadeh, R., & Rabiei-Dastjerdi, H. (2022). Chapter 5 - Assessment of machine learning algorithms in land use classification. In H. R. Pourghasemi (Ed.), *Computers in Earth and Environmental Sciences* (pp. 97–104). Elsevier. https://doi.org/https://doi.org/10.1016/B978-0-323-89861-4.00022-1

Krug, T., Kurz, W. A., Ogle, S., Raison, J., Schoene, D., Ravindranath Nagmeldin Elhassan, N. G., Heath, L. S., Higuchi, N., Kainja, S., Matsumoto, M., José Sanz Sánchez, M., Somogyi, Z., Carle, J. B., & Murthy, I. K. (n.d.). *Contributing Authors*.

Lee, L. X., Whitby, T. G., Munger, J. W., Stonebrook, S. J., & Friedl, M. A. (2023). Remote sensing of seasonal variation of LAI and fAPAR in a deciduous broadleaf forest. *Agricultural and Forest Meteorology*, *333*, 109389. https://doi.org/https://doi.org/10.1016/j.agrformet.2023.109389

Liepa, A., Thiel, M., Taubenböck, H., Steffan-Dewenter, I., Abu, I.-O., Singh Dhillon, M., Otte, I., Otim, M. H., Lutaakome, M., Meinhof, D., Martin, E. A., & Ullmann, T. (2024). Harmonized NDVI time-series from Landsat and Sentinel-2 reveal phenological patterns of diverse, small-scale cropping systems in East Africa. *Remote Sensing Applications: Society and Environment*, *35*, 101230. https://doi.org/https://doi.org/10.1016/j.rsase.2024.101230

Manson, S., Bonsal, D., Kernik, M., & Lambin, E. (2015). Geographic Information Systems and Remote Sensing. *International Encyclopedia of the Social & Behavioral Sciences*. https://doi.org/10.1016/B978-0-08-097086-8.91027-4

Maus, V., Câmara, G., Appel, M., & Pebesma, E. (2019). dtwSat: Time-Weighted Dynamic Time Warping for Satellite Image Time Series Analysis in R. *Journal of Statistical Software*, *88*(5), 1–31. https://doi.org/10.18637/jss.v088.i05

Miura, T., Huete, A. R., Yoshioka, H., & Holben, B. N. (2001). An error and sensitivity analysis of atmospheric resistant vegetation indices derived from dark target-based atmospheric correction.

Remote Sensing of Environment, *78*(3), 284–298. https://doi.org/https://doi.org/10.1016/S0034-4257(01)00223-1

Mulla, D. J. (2013). Twenty five years of remote sensing in precision agriculture: Key advances and remaining knowledge gaps. *Biosystems Engineering*, *114*(4), 358–371. https://doi.org/https://doi.org/10.1016/j.biosystemseng.2012.08.009

Pan, Z., Huang, J., Zhou, Q., Wang, L., Cheng, Y., Zhang, H., Blackburn, G. A., Yan, J., & Liu, J. (n.d.). *Mapping crop seasonality parameters using NDVI time-series derived from HJ-1 A/B data*. http://www.cresda.com/n16/index.html

Paris Agreement. (n.d.).

Petitjean, F., Kurtz, C., Passat, N., & Gançarski, P. (2012). Spatio-temporal reasoning for the classification of satellite image time series. *Pattern Recognition Letters*, *33*(13), 1805–1815. https://doi.org/https://doi.org/10.1016/j.patrec.2012.06.009

Ponce-Hernandez, R. (2004). *Assessing Carbon Stocks and Modelling Win-Win Scenarios of Carbon Sequestration Through Land Use Changes*. https://www.researchgate.net/publication/242563428

Post, W. M., & Kwon, K. (2008). Soil Carbon Sequestration and Land-Use Change: Processes and Potential. *Global Change Biology*, *6*, 317–327. https://doi.org/10.1046/j.1365-2486.2000.00308.x

Regional Innovation in Piedmont, Italy. (2021). OECD. https://doi.org/10.1787/7df50d82-en

Reichle, D. E. (2023). Timeline of anthropogenic alterations to the global carbon cycle. In D. E. Reichle (Ed.), *The Global Carbon Cycle and Climate Change (Second Edition)* (p. 284). Elsevier. https://doi.org/https://doi.org/10.1016/B978-0-443-18775-9.02011-8

Roh, T. W., Koo, J. C., Cho, D. S., & Youn, Y. C. (2014). Contingent feasibility for forest carbon credit: Evidence from South Korean firms. *Journal of Environmental Management*, *144*, 297–303. https://doi.org/10.1016/j.jenvman.2014.04.033

Roy, D. P., Lewis, P. E., & Justice, C. O. (2002). Burned area mapping using multi-temporal moderate spatial resolution data—a bi-directional reflectance model-based expectation approach. *Remote Sensing of Environment*, *83*(1), 263–286. https://doi.org/https://doi.org/10.1016/S0034-4257(02)00077-9

Sandra Brown. (1997). *FAO - Food and Agriculture Organization of the United Nations Rome, 1997*.

Sarmin, S., Hasan, Md. F., Hanif, A., Nur, A., & Shahin, A. (2024). *From Pixels to Policies : Remote Sensing for Compliance with Agriculture 4.0* (pp. 19–27).

Scarascia-Mugnozza, G., Oswald, H., Piussi, P., & Radoglou, K. (2000). Forest of the Mediterranean region: Gaps in knowledge and research needs. *Forest Ecology and Management*, *132*, 97–109. https://doi.org/10.1016/S0378-1127(00)00383-2

Song, J., & Wu, D. (2023). Modeling forest carbon sink trading with carbon credit using stochastic differential game. *Environmental Science and Pollution Research*, *30*(26), 68934–68950. https://doi.org/10.1007/s11356-023-26974-7

Verbesselt, J., Hyndman, R., Newnham, G., & Culvenor, D. (2010). Detecting trend and seasonal changes in satellite image time series. *Remote Sensing of Environment*, *114*(1), 106–115. https://doi.org/https://doi.org/10.1016/j.rse.2009.08.014

Wiegand, C. L., Richardson, A. J., Escobar, D. E., & Gerbermann, A. H. (1991). Vegetation indices in crop assessments. *Remote Sensing of Environment*, *35*(2), 105–119. https://doi.org/https://doi.org/10.1016/0034-4257(91)90004-P